Post-Translational Activation of Mmp2 by Mmp14 Is Triggered by Mechanical Signalling Through Piezo1 and Erk During Embryonic Growth in Zebrafish

by

Jillian E. Hickey

Bachelor of Science, University of New Brunswick, 2022

A Thesis Submitted in Partial Fulfillment
of the Requirements for the Degree of

Master of Science

in the Graduate Academic Unit of Biology

Supervisor: Bryan D. Crawford, Ph.D., Department of Biology

Examining Board: Jason Addison, Ph.D., Department of Biology, Chair
Alla Gagarinova, Ph.D., Department of Biology
Yang Qu, Ph.D., Department of Chemistry

This thesis is accepted by the Dean of Graduate Studies

THE UNIVERSITY OF NEW BRUNSWICK

April 2025

© Jillian E. Hickey, 2025

Abstract

To grow and change shape during development, wound healing and regeneration, multicellular tissues must remodel their extracellular matrix (ECM). The matrix metalloproteinases (MMPs) are the primary effectors of ECM remodeling. Using a transgenic zebrafish, we can visualize the activation of Mmp2 in intact embryos. Piezo1 is a stretch-sensitive, cation channel that is abundant in the epidermis of zebrafish embryos; I hypothesized that activation of Piezo1 triggers expression of Mmp14 via Erk signalling, resulting in Mmp2 activation. Consistent with this hypothesis, I observed increased *mmp14b* expression after treatment with the Piezo1 agonist Yoda1, and decreased *mmp14b* expression after treatment with either the Piezo1 inhibitor GsMTx4 or the MEK/ERK inhibitor PD0325901. I also found increased Mmp2 activation following treatment with Yoda1, and reduction of Mmp2 activation following treatment with GsMTx4 or PD0325901. These findings suggest a new link between stretching of epithelial tissues and the biochemical mechanisms of ECM remodeling *in vivo*.

Acknowledgements

First and foremost, thank you to my supervisor Dr. Bryan Crawford. Thank you for your support and guidance throughout both this thesis and my Honour's thesis. Thank you as well to all my lab mates. Kate Brown, Emily Moore, Matt Mabey, Kate McGregor, Nhu Trieu, Bianca Cruz, and Brennen Peters, thank you for all the help, the shenanigans, and for always making me excited to come to the lab. This research would not have been possible without any of you! I'd also like to thank NSERC for funding this research.

Thank you to my supervisory committee, Dr. Timothy Erickson and Dr. René Malenfant. Your edits and suggestions were invaluable. Thank you to Katie Theriault and everyone in the UNB aquatic facility for taking such great care of the fish. A big thank you to Samy Ahmed for dedicating so much time to cleaning tanks and getting the flow-through system back up and running! Thank you as well to everyone in the microscopy and microanalysis facility.

Finally, thank you to all my friends and family for supporting me and most importantly, thank you to my greatest mentor and the inspiration behind all my experiments, Iggy the lucky lab dragon.

Table of Contents

Abstract ii

Acknowledgements iii

Table of Contents iv

List of Tables vi

List of Figures vii

List of Symbols, Nomenclature, or Abbreviations ix

1. Introduction 1

1.1 Extracellular matrix 1

1.2 Matrix metalloproteinases 2

1.3 Regulation of MMP activity 3

1.4 Gelatinase A (Mmp2) 5

1.5 Epitope-mediated MMP activation (EMMA) assay 7

1.6 Piezo1 12

1.7 Calcium signalling 17

1.8 ERK signalling 18

2. Materials and Methods 23

2.1 Zebrafish husbandry and embryo collection 23

2.2 Chemical treatments 23

2.3 Epitope-mediated MMP activation (EMMA) assay 24

2.4 Immunofluorescence 24

2.5 HCR-RNA-FISH 25

2.6 Chorion trapping 26

2.7 RT gelatin zymography 26

2.8 Imaging and image processing 26

2.9 Quantification and statistical analyses 27

3. Results 32

3.1 Piezo1 activity regulates post-translational activation of EMMA-Mmp2 32

3.2 *mmp14b* expression is altered by Piezo1 activity 37

3.3 Erk inhibition reduces EMMA-Mmp2 activation and *mmp14b* expression 40

3.4 Trapping embryos in their chorion biases stretching of the epidermis 43

3.5 RT gelatin zymography 44

4. Discussion 46

4.1 Future work & conclusions 52

Bibliography 54

Curriculum Vitae

List of Tables

Table 2-1: Antibody dilutions and product information 25

List of Figures

Figure 1-1: General MMP structure 3

Figure 1-2: Activation of MMPs by cleavage of the propeptide domain 4

Figure 1-3: MT1-MMP dependent activation of MMP-2 7

Figure 1-4: Epitope-mediated MMP activation (EMMA) assay 9

Figure 1-5: EMMA-Mmp2 is activated in a patchwork-like pattern in the epidermis of growing zebrafish embryos 11

Figure 1-6: Piezo1 causes the membrane to curve into a cup shape 12

Figure 1-7: Yoda1 causes increased extension of the arm, resulting in activation of Piezo1 under sub-threshold stretch 15

Figure 1-8: Simplified ERK1/2 signalling cascade 20

Figure 2-1: Steps for quantifying 'hot-patches' of EMMA-Mmp2 activation 29

Figure 2-2: Steps for quantifying *mmp14b* expression 30

Figure 3-1: Piezo1 protein is abundant in the epidermis and accumulates in contexts in which Mmp2 activation occurs 32

Figure 3-2: Increasing Piezo1 activity results in increased activation of EMMA-Mmp2 34

Figure 3-3: Decreasing Piezo1 activity results in reduced activation of EMMA-Mmp2 35

Figure 3-4: Calcium signalling increases activation of EMMA-Mmp2 36

Figure 3-5: Increasing Piezo1 activity increases *mmp14b* expression 38

Figure 3-6: Decreasing Piezo1 activity reduces *mmp14b* expression..... 39

Figure 3-7: Inhibiting Mek/Erk signalling reduces EMMA-Mmp2 activation 41

Figure 3-8: Inhibiting Mek/Erk signalling reduces *mmp14b* expression..... 42

Figure 3-9: EMMA-Mmp2 activation is increased by stretch in the epidermis 44

Figure 3-10: Endogenous Mmp2 activation is increased slightly in embryos treated with Yoda1..... 45

Figure 4-1: Proposed pathway of Piezo1-dependent activation of Mmp2 via Mmp14 and Erk signalling..... 48

List of Symbols, Nomenclature, or Abbreviations

Throughout this thesis I have tried to be consistent with the nomenclature conventions for the species in question. Sometimes this is ambiguous but for example, zebrafish proteins are first letter capitalized, the rest lower case with no hyphen (e.g. Mmp2), but the convention for human proteins is all letters capitalized, with a hyphen (e.g., MMP-2). The following standard abbreviations are used throughout this thesis:

CaM – Calmodulin

CaMK – Calmodulin-dependent kinase

ECM – Extracellular matrix

EMMA – Epitope-mediated MMP activation assay

EMT – Epithelial-mesenchymal transition

ERK – General extracellular signal-related kinase

Erk – Zebrafish extracellular signal-related kinase

ERM – Embryo rearing medium

GsMTx4 – Grammostola mechanotoxin #4

eGFP – Enhanced green fluorescent protein

GPCR – G protein-coupled receptor

GPI – Glycosylphosphatidylinositol

HA – Hemagluttinin epitope tag

HCR-RNA-FISH – Hybridization chain reaction fluorescent in situ hybridization

hpf – Hours post-fertilization

Hsp70l – Heat-shock-70-like

ICK – Inhibitory cysteine knot

krt4 – Keratin 4 gene

LRP-1 – Low-density lipoprotein receptor-related protein-1

LUT – Lookup table

MAP – Mitogen-activated protein

MEK – Mitogen-activated protein kinase kinase

MMP – Matrix metalloproteinase

MMP-2 – Human gelatinase A protein

MMP2 – Murine gelatinase A protein

Mmp2 – Zebrafish gelatinase A protein

MMP-14 – Human MT1-MMP

MMP14 – Murine MT1-MMP

Mmp14 – Zebrafish MT1-MMP

mmp14b – Zebrafish MT1-MMP beta gene

MT1-MMP – Membrane type I matrix metalloproteinase

MSC – Mechanosensitive channel

PBS – Phosphate buffered saline

RECK – Reversion-inducing cysteine-rich protein with Kazal motifs

RFP – Red fluorescent protein

ROI – Region of interest

ROS – Reactive oxygen species

RTK – Receptor Tyr kinase

TAZ – Transcriptional coactivator with PDZ-binding motif

TIMP – Tissue inhibitor of MMP

YAP – Yes-associated protein

TRP – Transient receptor potential

1. Introduction

1.1 Extracellular matrix

The extracellular matrix (ECM) is a complex non-cellular structure that surrounds all tissues and organs. Composed primarily of collagen, fibronectin, laminin, and elastin, as well as about 200 other glycoproteins, and proteoglycans, the ECM is best known for its function as a scaffold for cells (Sekiguchi & Yamada, 2018). However, its roles go far beyond just maintaining tissue integrity. The ECM also provides elasticity, transmits biochemical and mechanical signals that regulate functions such as cell migration, proliferation, apoptosis, survival, and differentiation (Hu *et al*., 2022).

The extracellular matrix is also a dynamic structure that is constantly being remodeled by cells via ECM synthesis, degradation, reassembly, and post-translational modifications. Due to the importance of the ECM, these remodeling processes must be tightly regulated during development and wound healing, and to maintain tissue integrity during homeostasis in adults. Disruptions to the ECM can result in an overwhelming number of developmental defects and diseases in adults, including neurodegenerative disorders like Alzheimer's and diabetic retinopathy (Sun *et al*., 2021; Resnikoff *et al*., 2022); metabolic disorders like diabetes and obesity (Musale *et al*., 2023); inflammatory disorders like psoriasis, arthritis, and osteoporosis (Alcorta-Sevillano *et al*., 2020; Wagner *et al*., 2021; Wei *et al*., 2023); the pathological effects of viral infections like COVID-19 (Huang *et al*., 2023); cardiovascular diseases like arteriosclerosis (Di Nubila *et al*., 2024); fibrotic disorders (Cox & Erler, 2011); sleep and psychiatric disorders (Gisabella *et al*., 2021); and most notably the formation and metastasis of neoplastic tumours (Cox & Erler, 2011; Pickup *et al*., 2014).

1.2 Matrix metalloproteinases

The main effectors of ECM remodelling are matrix metalloproteinases (MMPs) and their endogenous inhibitors, the tissue inhibitors of metalloproteinases (TIMPs). MMPs are a family of zinc-dependent endopeptidases that degrade a wide variety of extracellular matrix proteins (Madzharova *et al*., 2019). There are approximately two dozen different MMPs; based on their structure and substrate specificity they are divided into six subfamilies: the collagenases (MMP-1, MMP-8, MMP-13), the gelatinases (MMP-2, MMP-9), the stromelysins (MMP-3, MMP-10, MMP-11), the matrilysins (MMP-7, MMP-26), membrane-type MMPs (MMP-14, MMP-15, MMP-16, MMP-17, MMP-24, MMP-25), and other non-classified MMPs (MMP-12, MMP-19, MMP-20, MMP-21, MMP-23, MMP-27, MMP-28) (Madzharova *et al*., 2019). While there is diversity amongst MMPs, almost all possess at least three structural components: an N-terminal secretory signal peptide, an autoinhibitory propeptide domain, and a catalytic domain (Figure1-1). Apart from MMP-7, MMP-23, and MMP-26, MMPs also possess a linker region and a hemopexin-like domain carboxyl to the catalytic domain, (Madzharova *et al*., 2019). The signal peptide targets MMPs to the secretory pathway, the propeptide domain possesses a conserved 'cysteine switch' motif that inhibits the catalytic activity, and the catalytic domain contains a highly conserved zinc-binding motif that is required for the proteolytic activity. The disordered hinge sequence links the catalytic domain to a hemopexin-like domain that is important for regulating substrate binding (Dufour *et al*., 2009). The majority of MMPs are secreted, consistent with their role as ECM remodelers, however the membrane-type MMPs are anchored to the membrane via either glycosylphosphatidylinositol (GPI) or a transmembrane domain

(Madzharova *et al*., 2019), and there are increasingly numerous reports of MMPs 'moonlighting' intracellularly, in which context their roles are still poorly understood (Fallata *et al*. 2019; Bassiouni *et al*. 2021).

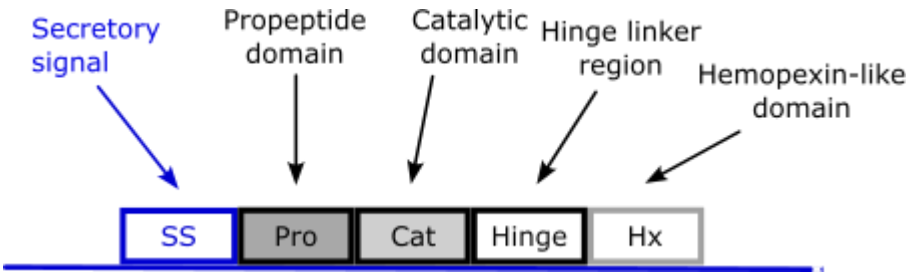

Figure 1-1: General MMP structure. The secretory signal (SS), propeptide domain (Pro), and catalytic domain are common to all MMPs. Apart from MMP-7, MMP-23, and MMP-26, all MMPs also contain a disordered hinge/linker region and hemopexin-like domain. The membrane-type MMPs also have additional membrane-spanning or membrane-tethering domains carboxyl to the hemopexin domain (not shown).

1.3 Regulation of MMP activity

Given the central role of MMP-mediated ECM-remodeling in developmental and physiological processes, MMP activity is tightly regulated to ensure that the correct ECM components are being degraded at the correct time and place. The first level of regulation is transcriptional. Genes encoding MMPs possess cis-regulatory elements regulating MMP transcription under control of growth factors, pro-inflammatory cytokines, hormones, and other signalling systems that respond to environmental cues (Madzharova *et al*., 2019). There are also multiple signalling pathways that allow for tissue-specific expression of MMPs. Epigenetic mechanisms such as DNA methylation and histone acetylation also regulate transcription of MMPs. However, with the notable exception of the uterine lining—which undergoes dramatic MMP-mediated remodelling during the normal menstrual cycle (Curry & Osteen, 2003; Gaide Chevronnay *et al*., 2012)—MMP expression is typically maintained at very low levels in homeostatic adult tissues.

There are multiple levels of post-transcriptional regulation as well. The majority of MMPs are secreted as inactive pro-enzymes or 'zymogens'. The cysteine switch motif in the propeptide domain interacts with the zinc ion in the catalytic domain and inhibits the proteolytic activity of the MMP. Activation of MMPs can result from chemical modification of the thiol group in the cysteine switch (e.g. by reactive oxygen species (ROS)) (Jacob-Ferreira & Schulz, 2013), or more commonly by the proteolytic cleavage and removal of the propeptide domain (Figure 1-2) (deAlmedia et al., 2022). Proteolytic cleavage requires the activity of an already active protease (e.g., other activated MMPs), and the network of proteolytic cross-activations that are responsible for this activation of MMPs is a subject of intense current interest (Mason & Joyce, 2011).

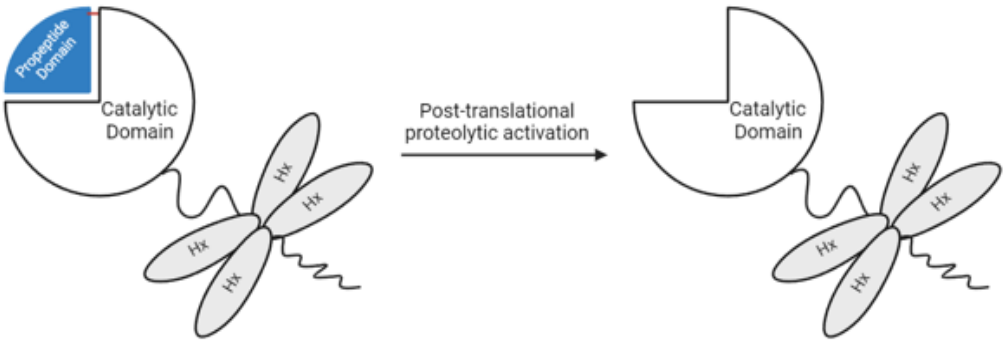

Figure 1-2: Activation of MMPs by cleavage of the propeptide domain. Removal of the propeptide domain exposes the zinc ion in the catalytic domain, causing the MMP to become proteolytically active.

Several MMPs cleave the propeptide domain of (and thereby activate) other MMPs *in vitro*, but far less is known about this process *in vivo* (Ra & Parks, 2007; Wyatt 2020; de Almeida *et* al., 2022). Once activated, the proteolytic activity of MMPs is reversibly modulated by interactions with substrates and competitive inhibition by

endogenous inhibitors such as TIMPs and reversion-inducing cysteine-rich protein with Kazal motifs (RECK) (Meng *et al*. 2008; Madzharova *et al*., 2019). MMP activity is also regulated by the cellular reuptake and degradation of MMPs from the extracellular fluid; for example, by endocytosis mediated by low-density lipoprotein receptor-related protein-1 (LRP-1) (Bres *et al*. 2019), but this final level of regulation has not been studied in detail.

1.4 Gelatinase A (Mmp2)

In this thesis, I elucidate a novel mechanism underlying the accumulation and activation of Mmp2 *in vivo* using the zebrafish model. MMP-2 (also known as gelatinase A and 72-kDa type-IV collagenase) along with MMP-9 (also known as gelatinase B) make up the gelatinase sub-family of MMPs. Gelatinase A has long been known to degrade denatured collagen (i.e. gelatin), as well as type IV and V collagen, proteoglycans, fibronectin, laminin and transferrin *in vitro* (Nagase *et al*., 1991). More recent work demonstrates that many MMPs, including gelatinase A, degrade non-matrix substrates, including intracellular substrates (Hadler-Olsen *et al*., 2015; Jobin *et al*., 2017; Xie *et al*., 2017; Gioia *et al*., 2018; Ali *et al*., 2021; Bassiouni *et al*., 2023; Maybee *et al*., 2023; Blascke de Mallo *et al*., 2024), suggesting roles for these proteases in broader contexts (Fallata *et al*., 2019). Nevertheless, most research continues to focus on the roles of MMPs in extracellular matrix remodeling, a context in which they certainly play a central role.

Research using mammalian tissue culture demonstrates that proMMP-2 can be activated through the cleavage of the MMP-2 propeptide domain by Membrane-type 1

MMP (a.k.a. MT1-MMP or MMP-14) (Strongin *et al*., 1993; Nishida *et al*., 2016). This MT1-MMP dependent activation of MMP-2 is mediated by TIMP-2. The C-terminal domain of TIMP-2 preferentially binds the hemopexin domain of inactive proMMP-2, while the N-terminal domain of the TIMP binds (and inhibits) the active site of an MT1-MMP, thus binding the proMMP-2 to the surface of the cell. Into this complex comes a second MT1-MMP, which interacts with the first via lateral interactions of their juxtamembrane hemopexin domains (Tochowicz *et al*., 2011). The proMMP-2 molecule is thus positioned by the bridging TIMP-2 such that its autoinhibitory propeptide is susceptible to attack by the uninhibited MT1-MMP (Strongin *et al.* 1993) (Figure 1-3). This generates a partially activated intermediate form of MMP-2 that undergoes autoactivation to become fully activated by an intermolecular autocleavage (Nishida *et al*., 2008). MMP-2 can also be activated by MMP-1, MMP-13, MMP-14, MMP-15, MMP-16, MMP-24, and MMP-25 (Laronha & Calderia, 2020), as well as by a variety of non-MMP proteases such as plasminogen, cathepsins, thrombospondins, in addition to non-enzymatic activation by reactive oxygen species, but there is remarkably little research published on these alternate mechanisms of gelatinase A activation (Monea *et al*., 2002; Zhang *et al*., 2002; Lee *et al*., 2003; Giusti *et al*., 2008).

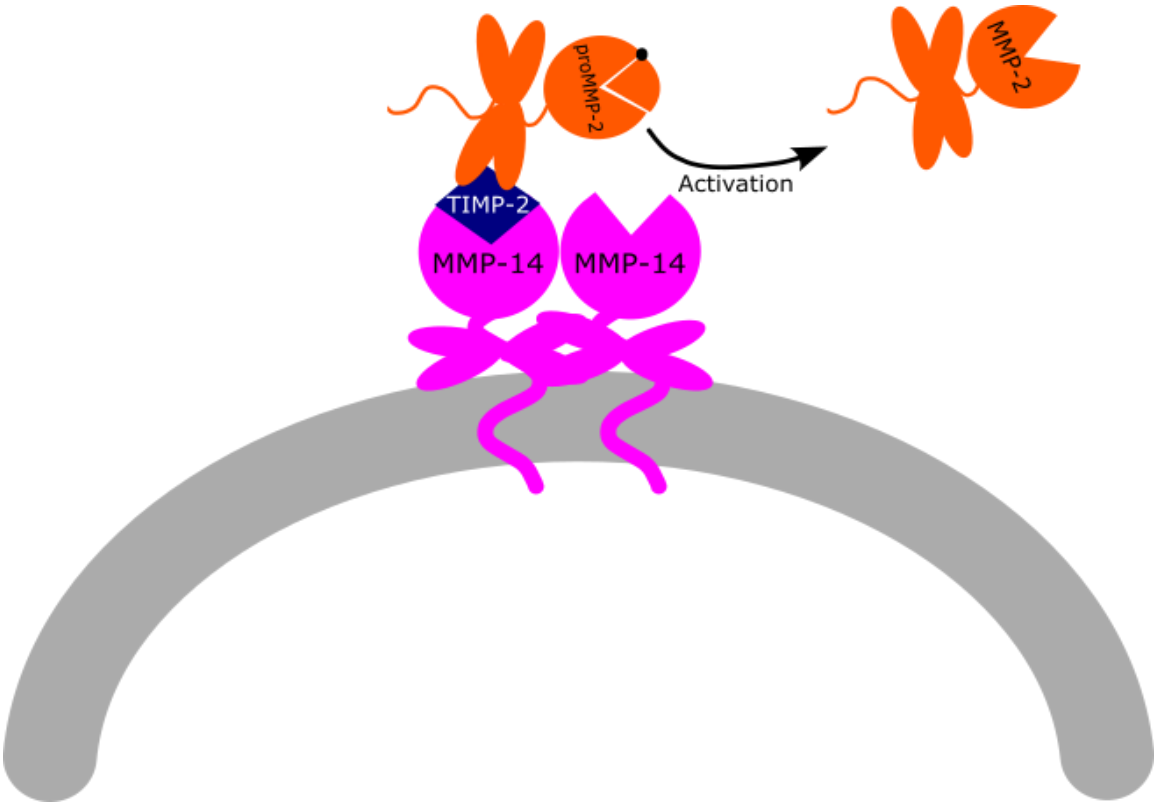

Figure 1-3: MT1-MMP dependent activation of MMP-2. MMP-14 dimerizes on the cell surface. One MMP-14 forms a complex with TIMP-2 and proMMP-2, facilitating the activation of MMP-2 by the adjacent free MMP-14.

1.5 Epitope-mediated MMP activation (EMMA) assay

Although *in vitro* activation of gelatinase A is well studied, very little of this complex process has been characterized or even demonstrated to occur *in vivo*. MMP activation is almost certainly affected by the native tissue context; therefore, *in vitro* methods may not provide biologically relevant or accurate information about this process. To better characterize both the mechanism(s) and regulation of MMP activation *in vivo*, Jeffery & Crawford (2018) developed the epitope-mediated MMP activation (EMMA) assay. The EMMA assay employs a novel catalytically inactive, doubly epitope-tagged reporter construct, consisting of the Mmp2 secretory signal, followed by a hemagglutinin (HA) epitope tag, the remainder of the zebrafish Mmp2 protein, and finally a C-terminal

enhanced green fluorescent protein (eGFP) sequence (Figure 1-4A). After translation, during which the N-terminal secretory signal is removed during transit into the endoplasmic reticulum through the Sec61 complex, the EMMA-Mmp2 product consists of the N-terminal propeptide domain tagged with HA and the C-terminal end of the catalytically inactive MMP tagged with GFP. Expression of the EMMA construct is driven by the zebrafish heat-shock-70-like (*hsp70l*) promotor, meaning its expression does not reflect that of the endogenous *mmp2* gene. However, using the *hsp70l* promotor yields relatively homogenous expression of the construct throughout the embryo, comparable to the more-or-less homogenous expression of the endogenous Mmp2 protein (Fallata *et al*., 2019). Therefore, significant accumulation/concentration of the EMMA-Mmp2 protein construct implies the activity of mechanisms(s) that bind/concentrate Mmp2 protein. To allow for normal embryo development, the catalytic site of the EMMA construct has been inactivated by converting an essential glutamate residue (E404) to an alanine. Consequently, we can detect endogenous Mmp2-processing mechanisms without causing the mis-regulation of ECM remodeling that results from overexpression of functional Mmp2.

The EMMA assay can be used to detect the activity of endogenous mechanisms that activate Mmp2 using immunofluorescence to detect colocalization, or lack thereof, of the HA and GFP epitopes. The colocalization of HA and GFP represents the full-length, unprocessed (inactive) form of the EMMA construct, whereas the localization of GFP alone indicates the propeptide domain has been proteolytically cleaved, representing the active form of the construct. Because the EMMA construct is catalytically inactive, this reveals the activity of endogenous Mmp2 activating mechanisms (rather than any

autoactivation) and allows us to visualize where and when mechanism(s) capable of cleaving the propeptide domain are functioning *in situ* (Figure 1-4).

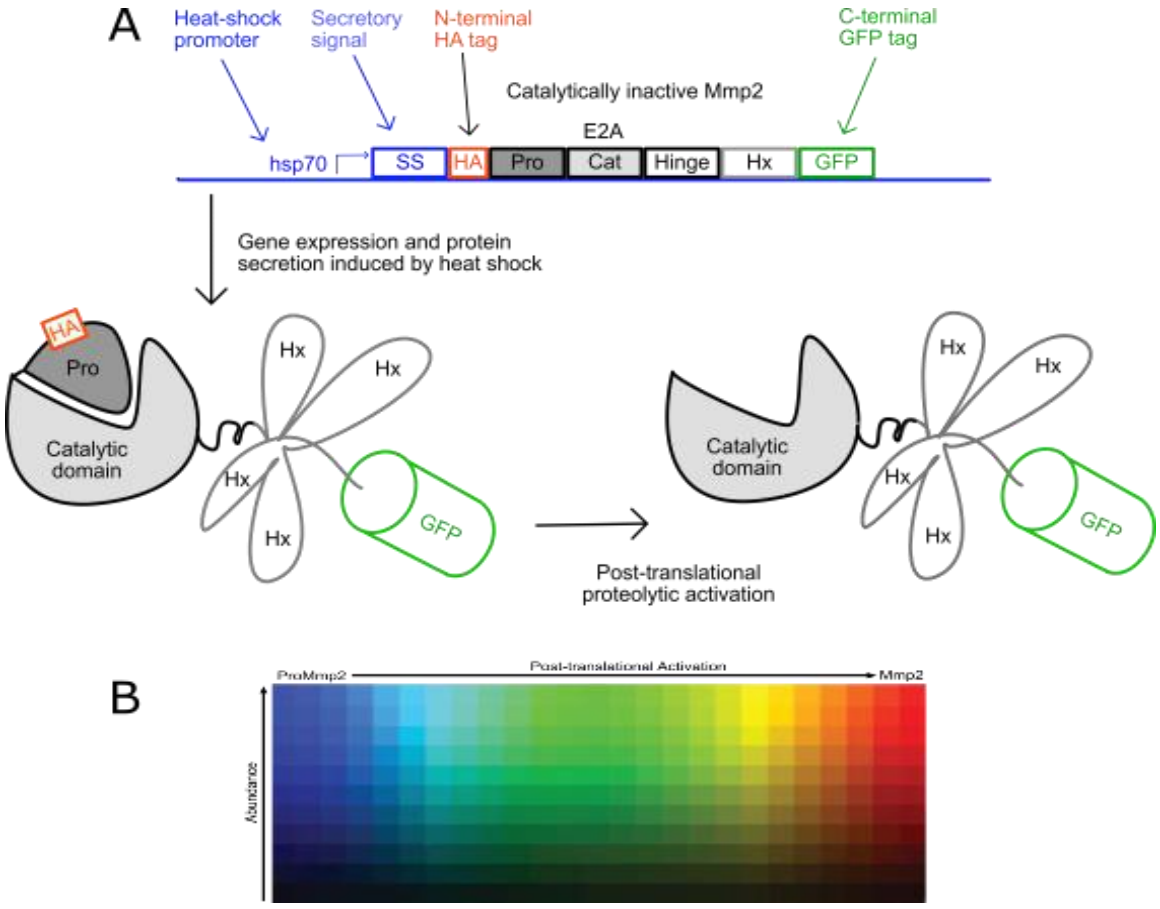

Figure 1-4: Epitope-mediated MMP activation (EMMA) assay. A) Schematic representation of the EMMA-Mmp2 reporter construct. **B)** The EMMA lookup table (LUT) used to show both activation and abundance data. Warmer colours represent greater activation, and brighter voxels indicate greater abundance.

Interestingly, if somewhat unfortunately, the initial efforts to generate an EMMA-Mmp2 reporter that could be used to visualize Mmp2 activation *in vivo* by fusing a red fluorescent protein (mCherry) to the propeptide were unsuccessful. This construct does not undergo post-translational proteolytic activation nor is it cleared by endogenous

mechanisms when expressed in zebrafish embryos; it persists as a full-length protein for over 24 hours without any detectable degradation or decrease in abundance (Jeffery & Crawford, 2018). Using the nine-amino-acid HA epitope to tag the propeptide precludes using the EMMA assay to characterize the post-translational activation of Mmp2 in real time. However, the EMMA construct with the HA epitope tag undergoes rapid processing giving rise to the expected sized intermediate and mature activation products, whereas the construct bearing a large mCherry domain fused to the propeptide remains inert and unchanged for over 24 hours *in vivo*. This strongly suggests that the processing of the HA tagged version of the EMMA construct represents the activity of *bona fide* Mmp2 processing mechanisms, and that these processing mechanisms are specifically selecting for the native Mmp2 propeptide.

Using the EMMA assay, Rachael Wyatt, a previous PhD student in the Crawford Lab, characterized the activation of EMMA-Mmp2 during normal embryonic development. Among other potentially developmentally important patterns of Mmp2 activation, Wyatt observed that EMMA-Mmp2 is activated in a patchwork-like pattern in the epidermis of growing zebrafish embryos (Wyatt, 2020; Wyatt & Crawford 2021). I have replicated these findings and consistently observe the same patchy activation (Figure 1-5).

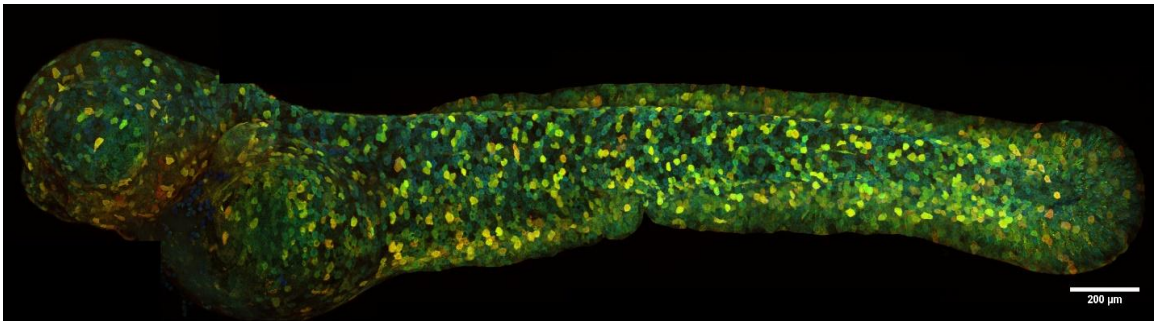

Figure 1-5: EMMA-Mmp2 is activated in a patchwork-like pattern in the epidermis of growing zebrafish embryos. Composite confocal projection of EMMA-processed 72 hours post-fertilization (hpf) embryo illustrating the patchy activation of EMMA-Mmp2 in the epidermis. Where the signal is brighter it means that the EMMA-Mmp2 construct is being bound and accumulating and where the signal is a warmer colour, a greater proportion of the EMMA-Mmp2 has undergone proteolytic activation.

This pattern of patches consisting of one or a few EMMA-Mmp2-activating cells, apparently randomly scattered throughout the epidermis, suggests a stochastic mechanism with lateral inhibition responding to a more-or-less homogeneous signal. We know that the epidermis of zebrafish embryos experiences stretching due to expansion of the underlying tissues (Silver *et al*., 2003; Chouhan *et al*., 2024). I hypothesize that this expansion triggers cells in the epidermis to bind and activate latent proMmp2 in their environment, thus causing local degradation of the basement membrane. This relieves the mechanical load locally, such that neighbouring cells experience less stretch and therefore do not activate their ECM-remodeling capacity. Such a mechanism, in which each epidermal cell responds independently to stretch, but in such a way that the response of one cell reduces the stretch experienced by nearby neighbours, would generate a patchwork-like pattern of Mmp2 activation while preventing large regions of the epidermis from degrading their ECM simultaneously. This raises the obvious question of how epidermal cells detect and respond to this stretch.

1.6 Piezo1

While there are a variety of mechanisms by which cells can detect and respond to stretch, Piezo1 is an ideal candidate for this role. Piezo1 is a cationic stretch-sensitive channel that transduces stretch by allowing calcium ions into the cell. In its closed conformation, Piezo1 adopts a propeller-like structure: a central pore surrounded by three large domains called arms or blades (Botello-Smith *et al*., 2019). Although it is possible to place a single domain of Piezo1 into the plane of the lipid membrane, the full Piezo1 trimer causes the membrane to curve into a cup shape (Figure 1-6).

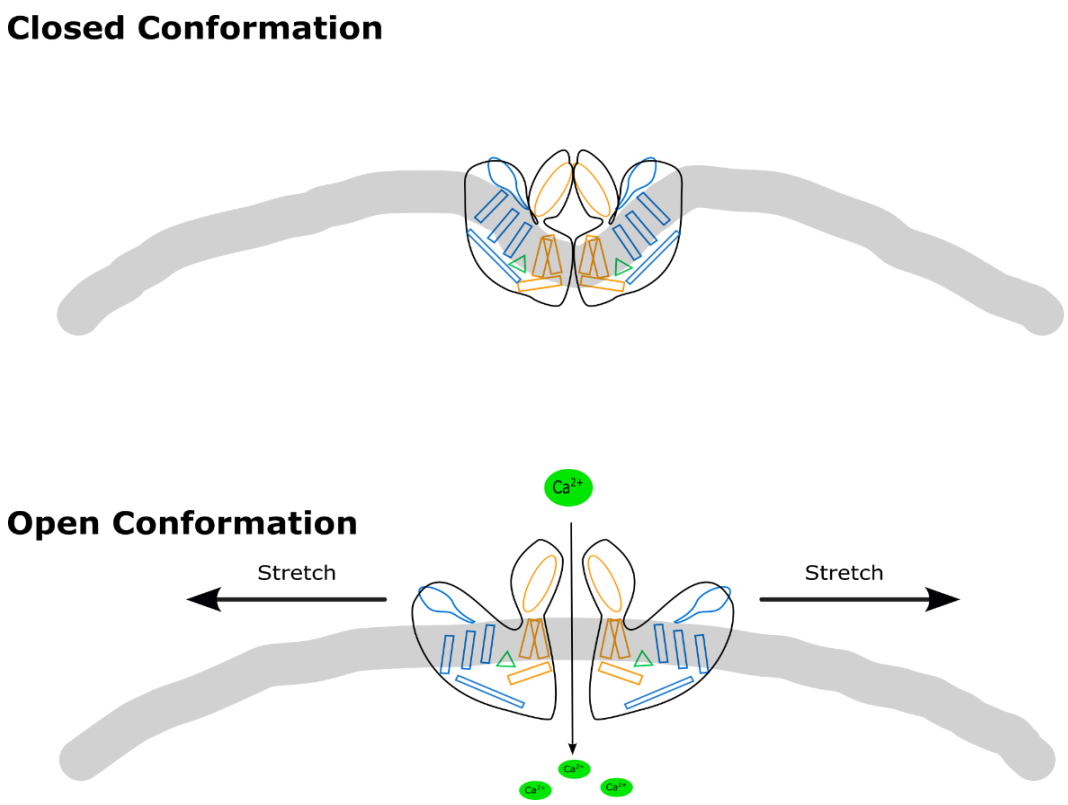

Figure 1-6: Piezo1 causes the membrane to curve into a cup shape. In its closed conformation, no cations can flow through the Piezo1 channel. When stretch is applied, it flattens out the membrane and pulls apart the Piezo1 trimer, allowing cations to flow into the cell (Qin *et al*., 2021).

This ability of Piezo1 to disrupt the planar shape of the lipid membrane allows the Piezo1 complex to respond to mechanical forces. When the membrane is stretched by a mechanical load, it causes the membrane to flatten out and become more planar. This flattening of the membrane causes the central pore of Piezo1 to open and selectively allow certain ions (such as calcium, sodium, and potassium) to pass through the pore and into the cell. The selectivity of Piezo1 for certain cations is most likely achieved by two rings of glutamate residues that flank either side of the central pore (Guo & MacKinnon, 2017). When the channel opens in response to mechanical forces, only cations that are small enough to fit through the glutamate rings, such as calcium, can enter the cell. This influx of positively charged ions contributes to the depolarization of the cell and ultimately allows for the conversion of mechanical stimuli on the membrane into an electrochemical response within the cell (Honoré *et al*., 2015).

Like other cation channels, Piezo1's ability to transport cations can be inhibited with gadolinium salts. Gadolinium ions do not directly interact with cation channels, they bind to the headgroup of phospholipids in the membrane. This pulls the headgroups closer together and causes the headgroups to become compact, resulting in a curvature in the lipid membrane (Ermakov *et al*., 2010). This curvature stabilizes the closed conformation of Piezo1 and other cation channels. Somewhat more specifically, grammostola mechanotoxin #4 (GsMTx4), a neurotoxin isolated from the venom of the Chilean rose tarantula *Grammostola spatulate*, inhibits mechanosensitive channels (MSCs) belonging to the Piezo and transient receptor potential (TRP) channel families (Gnanasambandam *et al*., 2017). GsMTx4 is a small peptide of 35 amino acids, built on a conserved inhibitory cysteine knot (ICK) backbone. Like all ICK peptides, GsMTx4 is

amphipathic with a hydrophobic face that promotes adsorption of the peptide to the lipid bilayer. Adsorption onto the bilayer is tension-dependent, and when GsMTx4 incorporates into the membrane it reduces the tension near the channel. When there is low tension on the membrane GsMTx4 resides near the surface of the membrane; however, when tension on the membrane increases, it promotes deeper insertion of GsMTx4 into the membrane, reducing the tension and preventing the activation of mechanosensitive channels such as Piezo1 (Gnanasambandam *et al*., 2017).

In 2015, the first agonist of Piezo1, dubbed 'Yoda1', was discovered by Syeda *et al*. Yoda1 is a small molecular agonist that activates Piezo1 through a molecular wedge mechanism (Botello-Smith *et al*., 2019). In the absence of mechanical force, the Piezo1 arm is in a flexed position; in the presence of a sub-threshold mechanical stimulus, the arm becomes slightly extended due to the partial flattening of the membrane, but not enough to open the pore. Yoda1 inserts itself between Repeats A and Repeat B, which causes increased extension of the arm (Figure 1-7). This results in the central pore of the Piezo1 protein opening in response to sub-threshold stimuli.

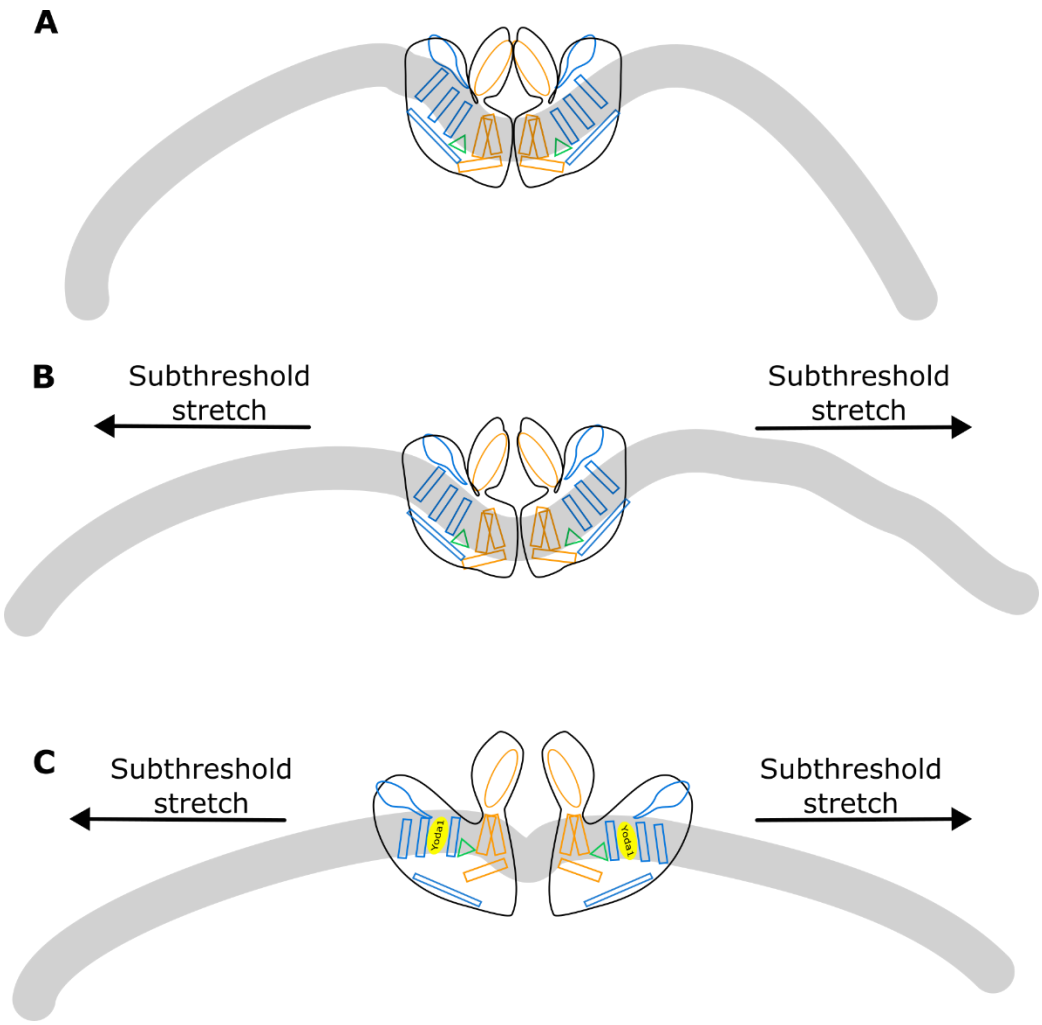

Figure 1-7: Yoda1 causes increased extension of the arm, resulting in activation of Piezo1 under sub-threshold stretch. A) Piezo1 is in its closed conformation in the absence of stretch. **B**) Subthreshold stretch results in partial flattening of the membrane but Piezo1 remains closed. **C**) Yoda1 causes extension of the Piezo1 arm, resulting in the opening of the channel in response to the same subthreshold stretch.

Since its discovery in 2010, there has been considerable research into the various roles of Piezo1, including the Nobel Prize–winning work of Ardem Patapoutian and David Julius (Martinac 2022). Amongst its many roles, Piezo1 regulates both cell division and cell extrusion in the epithelia of developing zebrafish embryos. Piezo1 regulates these two opposing processes by detecting different types of mechanical forces.

In response to stretch, Piezo1 increases intracellular calcium, which activates rapid cell division via extracellular signal-related kinase (ERK1/2) activity (Gudipaty *et al*., 2017). Piezo1-dependent cell extrusion is also mediated by calcium; however, cell extrusion is only initiated in response to crowding, rather than stretch (Gudipaty *et al*., 2017). How Piezo1 distinguishes stretch from crowding is not entirely understood, but the levels and localization of Piezo1, as well as the type of tension, may play a role in distinguishing these two different forces. In less dense areas that are prone to divide, Piezo1 localizes to the plasma membrane and the endoplasmic reticulum; however, in crowded regions where cell extrusion is more likely to occur Piezo1 develops into large cytoplasmic aggregates (Gudipaty *et al*., 2017). *In vitro*, Piezo1 signalling also triggers epithelial-mesenchymal transition (EMT) (i.e., the transition of epithelial cells into mesenchymal cells, a process central to both embryonic development and tumour metastasis), during which cells lose their polarity and cell–cell adhesion (He *et al*., 2022). Mechanical stretch regulates EMT marker expression, including the downregulation of E-cadherin (a cell–cell adhesion protein) as well as the upregulation of MMP2 and MMP9. Inhibition of Piezo1 by GsMTx4 antagonizes the downregulation of E-cadherin and the upregulation of MMP2 and MMP9 in response to stretch, indicating that Piezo1 is involved in regulating mechanical force-induced EMT (He *et al*., 2022). Both cell extrusion and EMT require the activity of MMPs, suggesting a link between Piezo1 (mechanical signalling) and MMP activation. In 2018, Kang *et al*. found that Piezo1 activity increases translocation of MT1-MMP to the plasma membrane of mouse lung endothelial cells *in vitro*; in cells depleted of Piezo1, membrane translocation of MT1-MMP tagged with a red fluorescent protein (RFP) was almost entirely inhibited. In 2023, Zhang *et al.* also

found that in hepatocellular carcinoma cells with depleted Piezo1, there was a significant reduction in *mmp14* expression. Because MT1-MMP activates other MMPs, including MMP-2 and MMP-9, these experiments suggest that Piezo1 may activate MMPs via an increase in MT1-MMP expression and presentation on the cell surface.

1.7 Calcium signalling

While Piezo1 allows all small cations (Na^+, K^+, Ca^{2+}, and Mg^{2+}) to pass through, it has a slight preference for Ca^{2+} (Drobnik *et al*., 2024). Of the small cations, calcium is also the most common and important second messenger. Calcium signalling regulates many cellular functions, including gene expression, vesicle fusion (e.g. neurotransmitter release), cell proliferation, and apoptosis (Prakriya, 2020). How calcium signalling regulates so many different pathways has been of intense research interest. Calcium signalling is downstream from several classes of ion channels, lipid signalling, as well as calcium pumps and transporters, and Ca^{2+} buffers. Calcium then regulates specific cellular functions by binding to different calcium-sensitive effector proteins such as calmodulin (CaM), which in turn translate the calcium signal into specific cellular responses (Prakriya, 2020).

Calmodulin is found in all eukaryotic cells and is the major regulator of Ca^{2+} signalling (Berchtold & Villalobo, 2013). Calmodulin interacts with and modulates many different target proteins and is involved in numerous cellular and physiological processes such as trafficking of vesicles between membrane-bound compartments of the cell (including the plasma membrane), cytoskeletal dynamics, cell cycle, apoptosis, phosphorylation/dephosphorylation of proteins, ion transport, and gene expression among many others (Berchtold & Villalobo, 2013). One group of calmodulin's downstream

targets are the calmodulin-dependent kinases (CaMKs) (Swulius & Waxham, 2008). Activation of CaMKs is typically dependent on the binding of Ca^{2+}/CaM, in which binding relieves the autoinhibitory mechanism that CaMKs display in the absence of Ca^{2+}/CaM (Swulius & Waxham, 2008). Once activated, CaMKs regulate gene transcription, apoptosis, vesicle mobilization, synaptic plasticity, ion channels, translation, muscle contraction, intracellular transport, and glycogen metabolism (Swulius & Waxham, 2008).

Calcium also regulates MMP expression and activity. In 2004, Mukhopadyay *et al*. found that increasing extracellular calcium results in an ERK1/2-dependent increase in MMP-9 expression. Interestingly, increasing calcium levels results in increased processing of pro-MMP-2 by promoting recruitment of TIMP-2 to MT1-MMP on the cell surface (Munshi *et al*., 2002), thereby facilitating the MT1-MMP-mediated activation of MMP-2 discussed in §1.4. These established roles of calcium signalling in the regulation of MMP expression and activation *in vitro* support a link between Piezo1 activity and MMP activation as I outline below.

1.8 ERK signalling

In the epidermis of the developing zebrafish embryo, I hypothesize that stretch increases calcium signalling through Piezo1, driving expression of *mmp14b* and consequently Mmp2 activation through extracellular signal-related kinase (Erk), some of which has been demonstrated *in vitro* (Takino *et al*., 2004; Chunderland & Seger, 2008; Sugimoto *et al*., 2023). Much like calcium, the mitogen-activated protein (MAP) kinase cascade, which culminates in activation of ERK, is a ubiquitous and well-studied signalling pathway that regulates processes such as proliferation, differentiation,

apoptosis, and stress response (Wortzel & Seger, 2011). Activation of the MAP kinase cascade is initiated by receptor Tyr kinases (RTKs), G protein-coupled receptors (GPCRs), ion channels, and other membrane receptors. The signal is then transmitted by recruiting SH2-domain containing adaptor proteins (such as Grb) that recruit guanine nucleotide exchange factors (like Sos) that induce the activation of the membrane-tethered small GTPase Ras. Ras activates the Raf protein kinases, which transmit the signal by phosphorylating mitogen-activated protein kinase kinase (MEK1/2). MEK1/2 then activates its only known substrate ERK1/2 via phosphorylation (Figure 1-8) (Wortzel & Seger, 2011). Once activated, ERK phosphorylates various targets in the cytoplasm, as well as the nucleus, which in turn regulate processes such as transcription and vesicular trafficking (Chunderland & Seger, 2008).

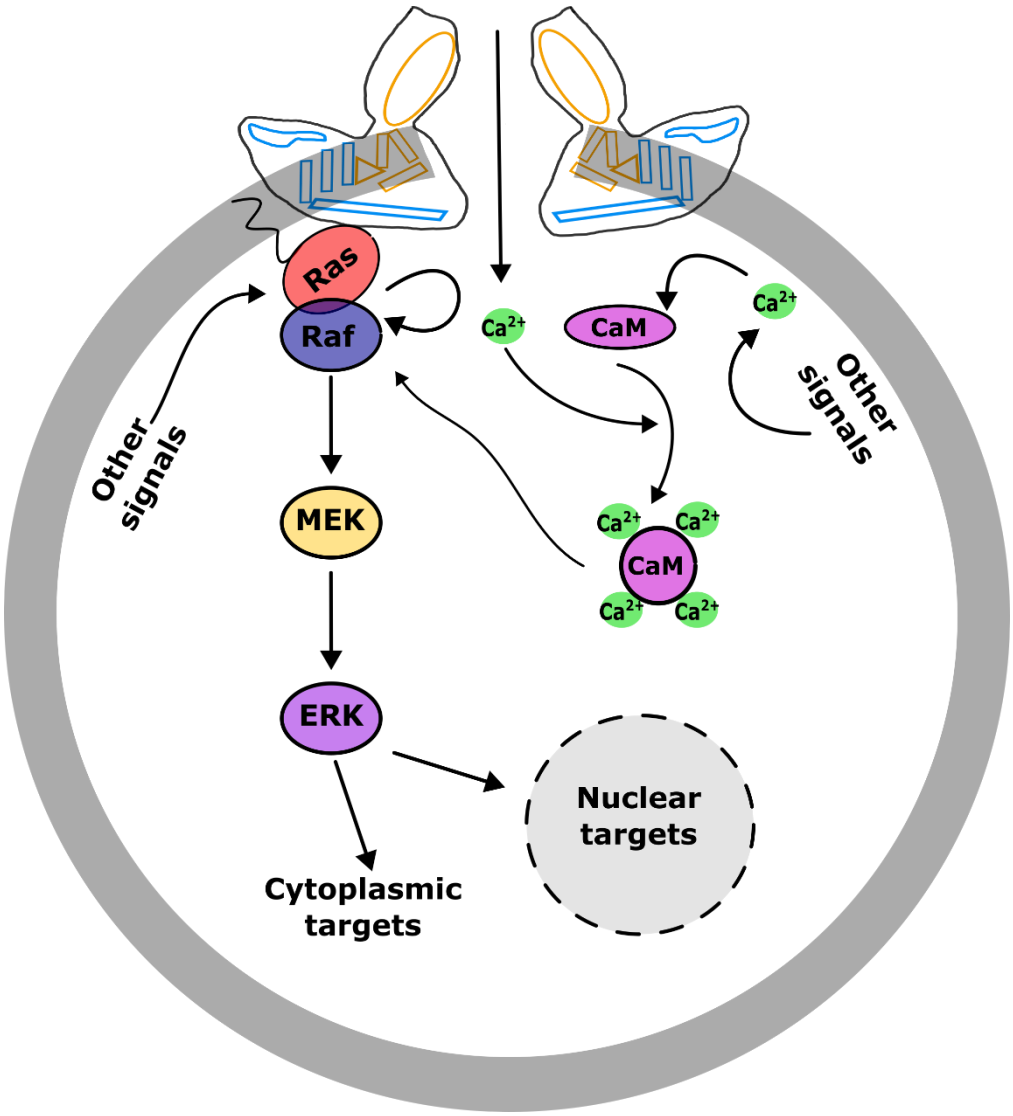

Figure 1-8: Simplified ERK1/2 signalling cascade. Increased intracellular calcium regulates adapter proteins such as calmodulin, which in turn activate Raf (Salzano *et al*., 2012). Once activated, ERK regulates both cytoplasmic targets and nuclear targets after translocation into the nucleus.

Increasing intracellular calcium via release from internal stores or through membrane calcium channels activates the ERK cascade (Chuderland & Seger, 2008). Mechanisms that activate the cascade include activation of the calcium-affected kinase PYK2, activation of Ras via increased activity of the guanine nucleotide exchange factor Ras-GRF and inhibition of the GTPase activating protein Ras-GAP, as well as activation

of calmodulin-dependent kinases I and II. Calcium also regulates the ERK cascade by modulating the protein–protein interactions that involve ERK, which in turn modifies the subcellular localization of ERK (Chunderland & Seger, 2008). Piezo1 activity also regulates ERK activity more directly: Piezo1 possesses an R-Ras-binding domain that more specifically targets the activation of the cascade, culminating in ERK activation by the influx of calcium (Sugimoto *et al*., 2023). Very recently, Ramkumar *et al.* (2025) showed that Erk activity is activated by stretch in the epidermis of zebrafish, adding *in vivo* support for this model.

Furthermore, it appears that ERK is part of a feedback loop that drives MMP expression and activation; MT1-MMP increases MEK1/2 phosphorylation and ERK activation through an unknown but TIMP-2 dependent signalling pathway (Sounni *et al*., 2011), and ERK signalling in turn increases MT1-MMP expression (Tanimura *et al*., 2003; Takino *et al*., 2004). Increasing ERK activity also results in increased MT1-MMP-dependent processing of pro-MMP-2 to active MMP-2 *in vitro* (Takino *et al*., 2004).

In this thesis, I show that Piezo1 activity triggers expression of *mmp14b* expression via calcium-dependent Erk signalling, resulting in patches of EMMA-Mmp2 activation in the epidermis. I observe increased *mmp14b* expression in the epidermis using hybridization chain reaction (HCR) following treatment with Yoda1, and I observe decreased *mmp14b* expression following treatment with GsMTx4 or the MEK/ERK pathway inhibitor PD0325901. I also observe increased EMMA-Mmp2 activation patches following treatment with Yoda1, and reduction of EMMA-Mmp2 activation following treatment with GsMTx4 or PD0325901. Finally, I provide some preliminary results showing that mechanical deformation of the embryo affects Mmp2 activation as

predicted by this model. These findings provide a new link between mechanical stretching of epithelial tissues and the biochemical mechanisms of ECM remodeling *in vivo*, shedding light on the feedback mechanisms regulating tissue morphogenesis in vertebrates.

2. Materials and Methods

2.1 Zebrafish husbandry and embryo collection

Zebrafish (*Danio rerio*) were maintained at 28.5 °C following a 14 h light/10 h dark cycle. Fish were fed dry pellets (Skretting) twice daily. The strains used were wild-type (Tübingen) and EMMA-Mmp2 (*Tg(hsp70l:SS-HA-ATTB-1-mmp2_E404A-ATTB2-EGFP*) (Jeffrey & Crawford, 2018). Embryos were collected by natural spawning over marbles and grown in embryo rearing medium (ERM:13.7 mM NaCl, 0.5 mM KCl, 0.13 mM Na_2HPO_4, 0.22 mM KH_2PO_4, 1.3 mM $CaCl_2$, 1 mM $MgSO_4$, 4.2 mM $NaHCO_3$, pH 7.4). All work in this study on zebrafish adults and embryos was done in accordance with and under the supervision of the University of New Brunswick Animal Care Committee and the Canadian Council on Animal Care.

2.2 Chemical treatments

Aliquots of Yoda1 (448947-81-7, Tocris, dissolved at 30 mM in DMSO), GsMTx4 (HB1161, Hello Bio, dissolved at 100 µM in dH_2O), calcium ionophore A23187 (25665-69-7, Sigma, dissolved at 50 mM in DMSO), and MEK inhibitor PD0325901 (391210-10-9, Stemcell Technologies, dissolved at 1 mM in DMSO) were stored at -20˚C.

Embryos treated with Yoda1, A23187 and PD0325901 were exposed by bathing in these compounds at 3 µM, 50 µM or 30 µM, respectively, alongside vehicle controls treated identically. Embryos treated with Yoda1 were manually dechorionated at 48 hours post-fertilization (hpf) and incubated overnight at 28.5˚C before analysis by EMMA assay at 72 hpf. Embryos treated with A23187 and PD0325901 were exposed by bathing for 4.0 hours starting at 72 hpf. For GsMTx4 treatments, embryos were

anesthetized in tricane and microinjected with GsMTx4 diluted 1:1 with sterile-filtered danieau buffer (17.4 mM NaCl, 0.21 mM KCl, 0.12 mM $MgSO_4$, 0.18 mM $Ca(NO_3)_2$, 1.50 mM HEPES Buffer, pH 7.6; 50 µM GsMTx4 final) (or sham injected with danieau buffer alone) at 72 hpf, and allowed to recover for 2 hours in ERM before analysis by EMMA assay.

2.3 Epitope-mediated MMP activation (EMMA) assay

Expression of the EMMA construct was induced by heat-shocking in a hot water bath. Embryos in 2 mL microfuge tubes were floated in the water bath at 28.5˚C. The temperature was ramped up to 38˚C over 8 minutes and then held at 38˚C for 30 min, followed by cooling to 28.5°C over 12 minutes. Embryos were allowed to recover, express and proteolytically process the EMMA reporter for 4 hours at 28.5˚C before fixation in 4% formaldehyde (Electron Microscopy Sciences) in 0.1x Phosphate Buffered Saline (PBS) overnight at 4˚C. Immunofluorescence was then used to detect the colocalization, or lack thereof, of the HA and GFP tags (see §2.4). Following immunostaining, embryos were mounted, imaged, and processed according to §2.8.

2.4 Immunofluorescence

Embryos were washed 3x15 minutes at room temperature to remove fixative; they were then incubated in blocking buffer (PBS with 0.1% Triton X-100 (PBS-Tx) and 5% BSA) overnight at 4˚C. Blocked embryos were incubated in 1˚ antibodies (Table 2-1) diluted in blocking buffer overnight at 4˚C, washed 3x15 min in PBS-Tx, then incubated in 2˚ antibodies (Table 2-1) overnight at 4˚C, before finally being washed 3x15 min in PBS-Tx and mounted for imaging.

Table 2-1: Antibody dilutions and product information.

Antibodies	Dilution	Source
Mouse anti-GFP (C-terminal tag for EMMA)	1:1000	11814460001, Roche
Rat anti-HA (N-terminal tag for EMMA)	1:1000	11867423001, Roche
Rabbit anti-Piezo1	1:500	NBP1-78446SS, Novus
Goat anti-mouse Alexa488 (EMMA 2˚)	1:1000	A11001, Life Technologies
Goat anti-rat Alexa 555 (EMMA 2˚)	1:1000	A21434, Invitrogen
Goat anti-rabbit Alexa 488	1:1000	A11008, Life Technologies

2.5 HCR-RNA-FISH

HCR-RNA-FISH (hybridization chain reaction or HCR) was conducted according to the Molecular Instruments procedure (MI-Protocol-RNAFISH-Zebrafish, 2018), with the exceptions that embryos were not treated with proteinase K and the *mmp14b* probe was used at 8 nM (double the recommended concentration), after consultation with Molecular Instruments in order to reduce autofluorescence and increase signal. After HCR, embryos were treated with Vector TrueVIEW autofluorescence quenching solution (SP-8400, Vector Laboratories) for 30 minutes to reduce autofluorescence before imaging.

2.6 Chorion trapping

Live embryos were trapped in their chorions by immersing 24 hpf embryos in 0.0006% bleach for 5 minutes (Hall *et al*., 2023). Embryos were washed 3X5 minutes in ERM following bleaching, and ERM was changed daily until fixation. At 48 hpf embryos were heat-shocked and then fixed in 4% formaldehyde 4 hours post-heat-shock. Embryos were manually dechorionated following fixation and then processed for the EMMA assay. Control embryos were treated the same apart from being manually dechorionated immediately after bleaching.

2.7 RT gelatin zymography

Real-time gelatin zymography was conducted according to the procedure by Hadler-Olsen & Winberg, 2019 with minor adjustments (gelatin was dialyzed after MDPF-conjugation but used directly without intermediate lyophilization for logistical reasons). Homogenates of embryos treated with 3 µM Yoda1, 30 µM PD0325901, and their respective controls, were run on the gel. Homogenates were made by flash-freezing embryos in non-reducing SDS-PAGE sample buffer with liquid nitrogen, followed by pulverization. Embryo homogenates were then collected and stored at -20°C.

2.8 Imaging and image processing

Fixed embryos were imaged with a Leica SP-8 Confocal Laser Scanning system mounted on a DMi8 inverted microscope fitted with a 25× 0.95NA water-immersion lens using 2 µm step sizes. 488 nm and 552 nm lasers excited the Alexa 488, Alexa 555, and Alexa 546 fluorophores. Detector gain was adjusted to fill the dynamic range of the HyD detector, avoiding saturation and zero values; comparable embryos were imaged using identical settings.

Raw EMMA assay images were processed using FIJI (V1.54p) (Schindelin *et* al., 2012), with custom macros developed by Rachel Wyatt (Wyatt, 2020), to illustrate both the total abundance of GFP and ratio of GFP:HA signal intensity as brightness and colour, respectively (Wyatt & Crawford, 2021). Because the proteolytically processed construct yields purely green signal, and the unprocessed construct yields a yellow signal (i.e. both green and red), the visual contrast between these signals is increased by mapping the ratios of these signals to a custom EMMA lookup table (LUT). The proportion of the EMMA-Mmp2 reporter that has been activated in any given voxel is illustrated by mapping the ratio of GFP:HA signal intensity to the EMMA LUT with higher ratios (i.e. more activation) assigned as the red end of the spectrum and lower ratios (i.e. less activation) assigned the blue (Wyatt & Crawford, 2021) (Figure 1-4B). Gaussian smoothing was used to reduce noise and to reduce false signals generated by slight variations in the *x*, *y* positions of signals in the green and red channels.

All images were z-projected in either sum slices or max intensity mode and stitched into high-resolution composites using the Pairwise Stitching plugin (Preibish *et al*., 2009).

2.9 Quantification and statistical analyses

EMMA-Mmp2 activation was quantified using colour thresholding in FIJI to select only the active EMMA-Mmp2 by including pixels only at the red end of the spectrum. Regions of interest (ROIs), including only fin-fold epidermis were selected, both to eliminate confounding effects of limited drug penetration in bathing experiments, and to exclude neural, mesodermal and other tissues that may not be subjected to similar mechanical forces during elongation and growth of the embryo. Finally, I used the

"analyze particles" function to determine the % Area of the ROIs exceeding the colour threshold representing EMMA-Mmp2 activation (Figure 2-1). Comparable embryos were analyzed using the same thresholding parameters. To compare between experimental treatments and correct for day-to-day variations, % Area values were normalized by dividing each value by the mean of control values, such that the mean % Area of activated EMMA-Mmp2 is always 1.0 in control embryos.

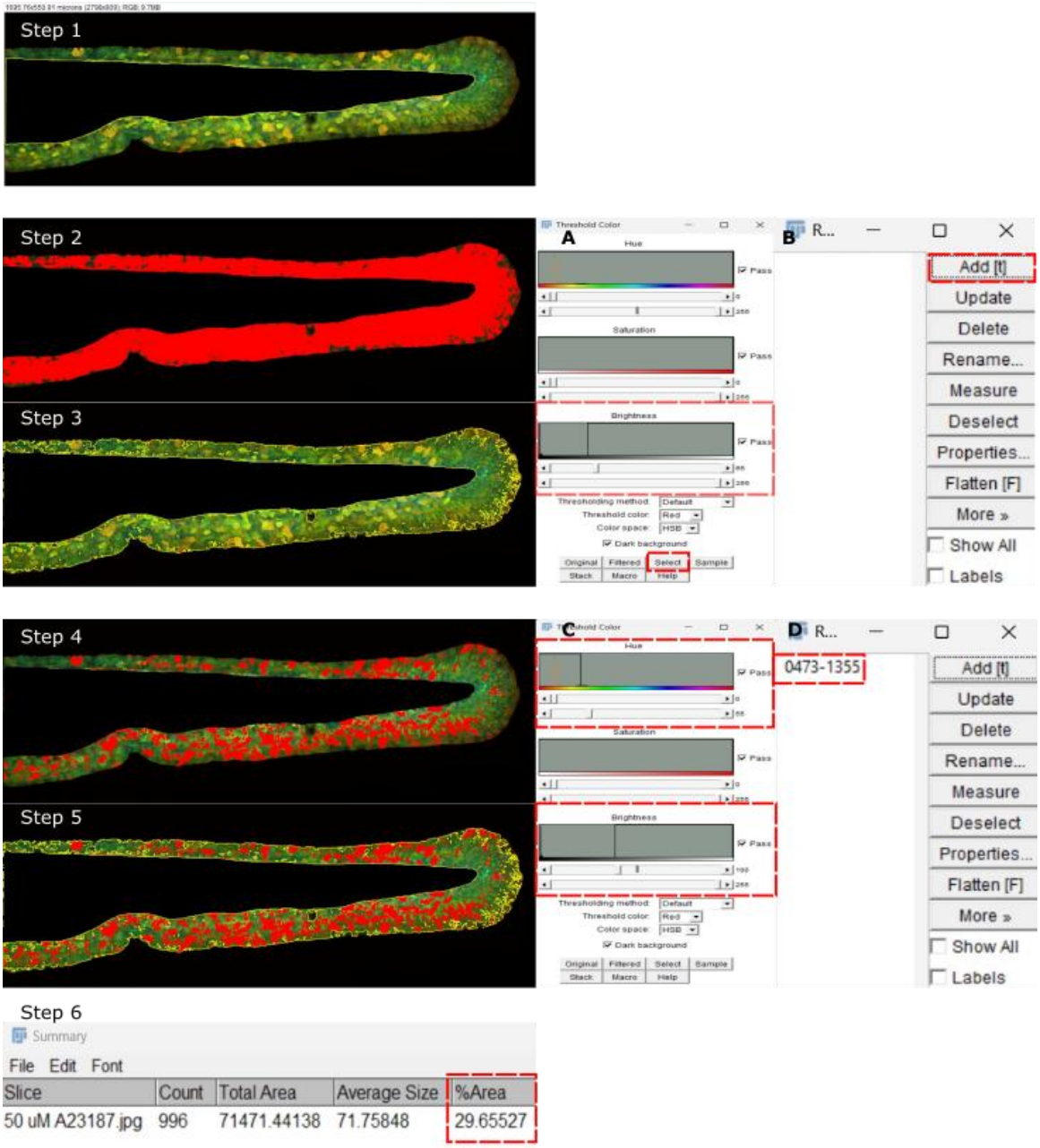

Figure 2-1: Steps for quantifying 'hot-patches' of EMMA-Mmp2 activation. Step 1: Use freehand select tool to outline and delete the mesoderm, leaving only fin-fold epidermis. Step 2: Adjust brightness in colour thresholding to select ROI (**A**), excluding any holes that may have resulted during imaging. Step 3: Click select at the bottom of the colour thresholding panel (**A**) and then add it as a region of interest using ROI manager (**B**). Step 4: Adjust hue and brightness in colour thresholding panel until only the patches of active EMMA-Mmp2 are selected (**C**). Step 5: Add the ROI back to the image using the ROI manager (**D**). Step 6: Calculate the % Area using the "analyze particles" function.

mmp14b expression was quantified similarly but using greyscale thresholding rather than colour thresholding (Figure 2-2). ROIs were again used to select the fin fold epidermis and the % Area of *mmp14b* hybridization signal was measured. All values were again normalized to the controls.

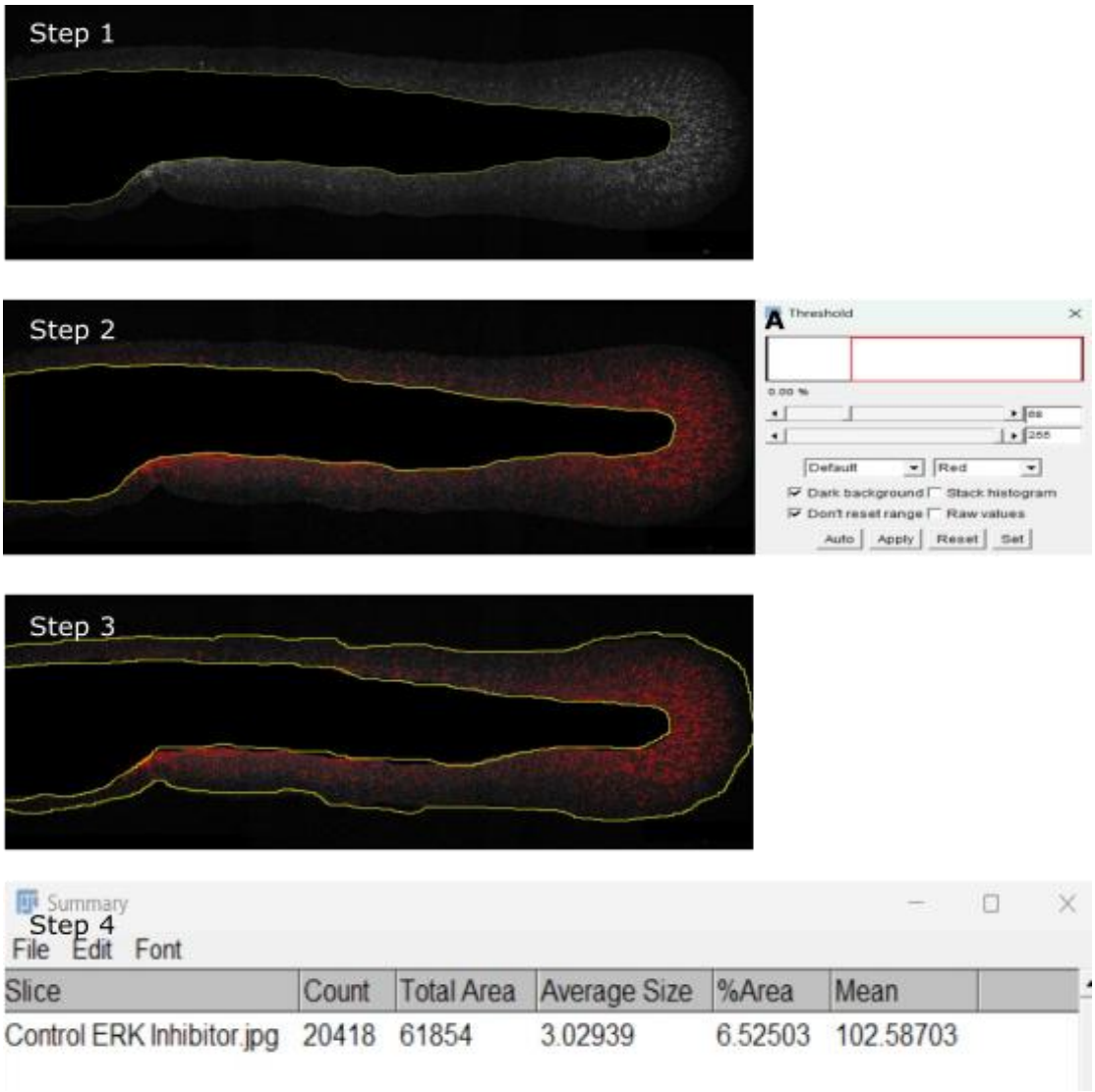

Figure 2-2: Steps for quantifying *mmp14b* expression. Step 1: Use the freehand select tool to outline and delete the mesoderm, leaving only fin-fold epidermis. Step 2: Use thresholding to adjust brightness such that the bright dots that shows where *mmp14b* RNA is present are selected (**A**). Step 3: Use the freehand select tool to outline the region of interest (i.e., the fin-fold epidermis). Step 4: Calculate the % Area using the "analyze particles" function.

The normalized fractional area of activated EMMA-Mmp2 and *mmp14b* expression of control and treatment embryos were compared using Welch's t-test in R (V4.3.1) (R Core Team, 2023). To assess that the data was normally distributed the data was visualized using a qqPlot and a Shapiro-Wilk test was performed.

3. Results

3.1 Piezo1 activity regulates post-translational activation of EMMA-Mmp2

Because Piezo1 is stretch-activated, I wondered if Piezo1 might be involved in the regulation of post-translational Mmp2 activation in the epidermis, which we know is subjected to stretch by the growth of the underlying tissues (Ramkumar *et al.* 2025). Using immunofluorescence, I found that Piezo1 protein accumulates in a wide variety of tissues in which Mmp2 activation occurs, notably the vasculature, craniofacial cartilage, neuromasts, myofibrils, fin-fold mesenchyme, and throughout the epidermis (Figure 3-1).

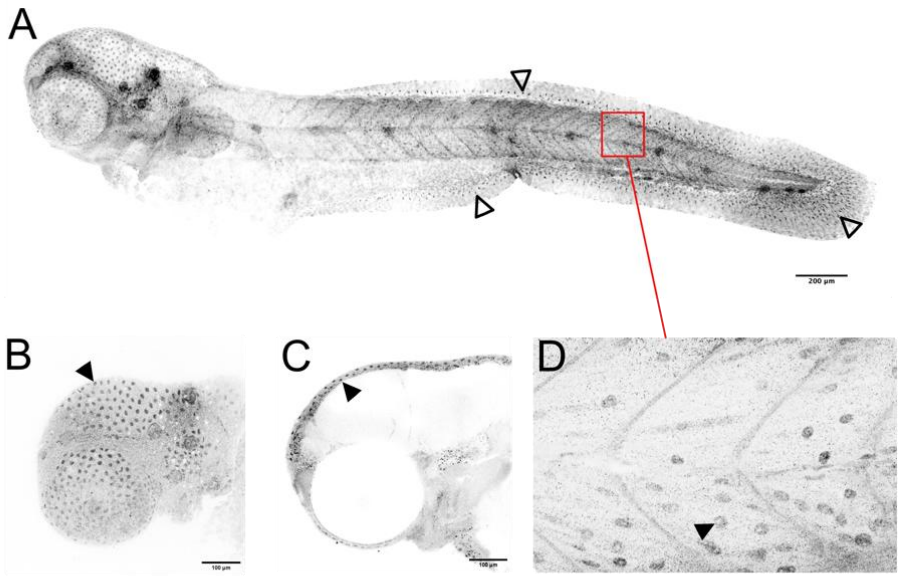

Figure 3-1: Piezo1 protein is abundant in the epidermis and accumulates in contexts in which Mmp2 activation occurs. A) Composite confocal projection of a 72 hpf embryo stained with anti-Piezo1. Piezo1 accumulates broadly throughout the epidermis, myotome boundaries, neuromasts, and is strongly expressed in the fin-fold mesenchyme (open arrowheads). Scale bar = 200 µm. **B** & **C**) Higher magnification views of Piezo1 immunostaining in the epidermis of the head, showing abundant staining in the nuclei (arrowheads). Scale bar = 100 µm. **D**) Higher magnification view of Piezo1 immunostaining in the myotomes, illustrating accumulation at the myotendenous junctions and nuclear envelope (arrowhead).

To investigate the role of Piezo1 in the regulation of Mmp2 activation, I treated EMMA-Mmp2 embryos with the Piezo1 agonist Yoda1 (Syeda *et al*., 2015), and microinjected embryos with the Piezo1 antagonist GsMTx4 (Bae *et al*., 2011). I found a significant increase in EMMA-Mmp2 activation in the epidermis of embryos treated with Yoda1 (Figure 3-2) and a significant decrease in EMMA-Mmp2 activation in embryos injected with GsMTx4 (Figure 3-3). To verify that these chemical treatments were altering EMMA-Mmp2 activation and not altering the expression of the transgene, I imaged live EMMA-Mmp2 embryos bathed in either Yoda1 or vehicle control, as well as embryos microinjected with either GsMTx4 or danieau buffer (sham injected), 4 hours post-heat-shock using a Leica M205A motorized epi-fluorescent stereo dissecting microscope, to detect the GFP on the carboxyl end of the EMMA-Mmp2 construct. I then measured the mean greyscale values of the embryos using FIJI and found there to be no significant difference in Yoda1-treated embryos or GsMTx4-injected embryos compared to their respective controls (Figure 3-2 C&D and Figure 3-3 C&D). This indicates that the expression of the transgene is not significantly altered by the treatments.

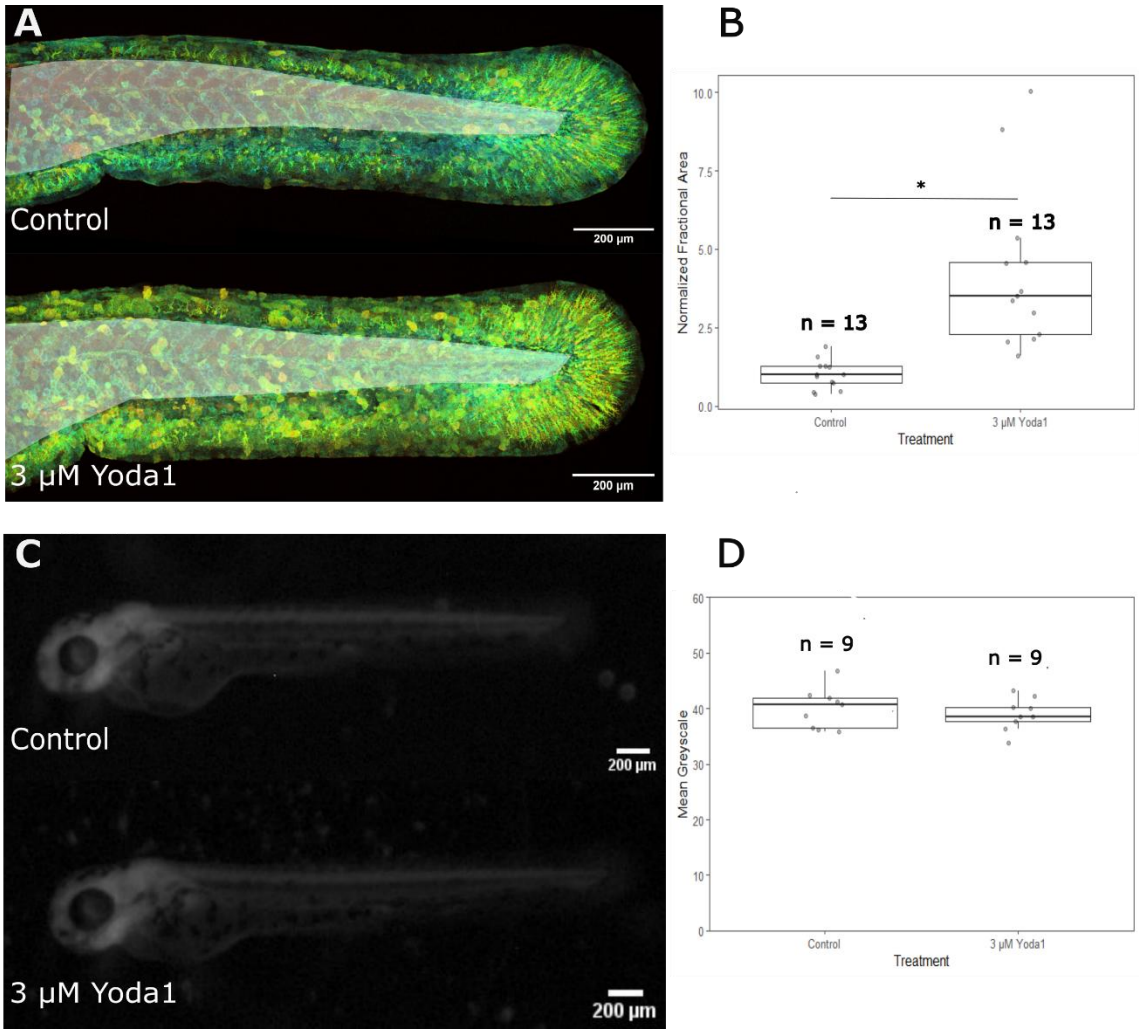

Figure 3-2: Increasing Piezo1 activity results in increased activation of EMMA-Mmp2. A) Composite confocal projection of EMMA-processed 72 hpf embryos incubated in vehicle control (top) or 3 µM Yoda1 (bottom). Shaded area indicates area excluded from quantification. **B)** Quantification of EMMA-Mmp2 activation in the epidermis using colour thresholding ($p < 0.001$, $t = -4.434$, d.f. = 12.73, mean (control) = 1.00 ± 0.449, mean (3 µM Yoda1) = 4.218 ± 2.575). **C)** Live 72 hpf embryos incubated in vehicle control (top) or 3 µM Yoda1 (bottom). **D)** Quantification of GFP intensity obtained by measuring mean greyscale values ($p = 0.489$, $t = 0.709$, d.f. = 15.27, mean (control) = 40.033 ± 3.589, mean (3 µM Yoda1) = 38.943 ± 2.881).

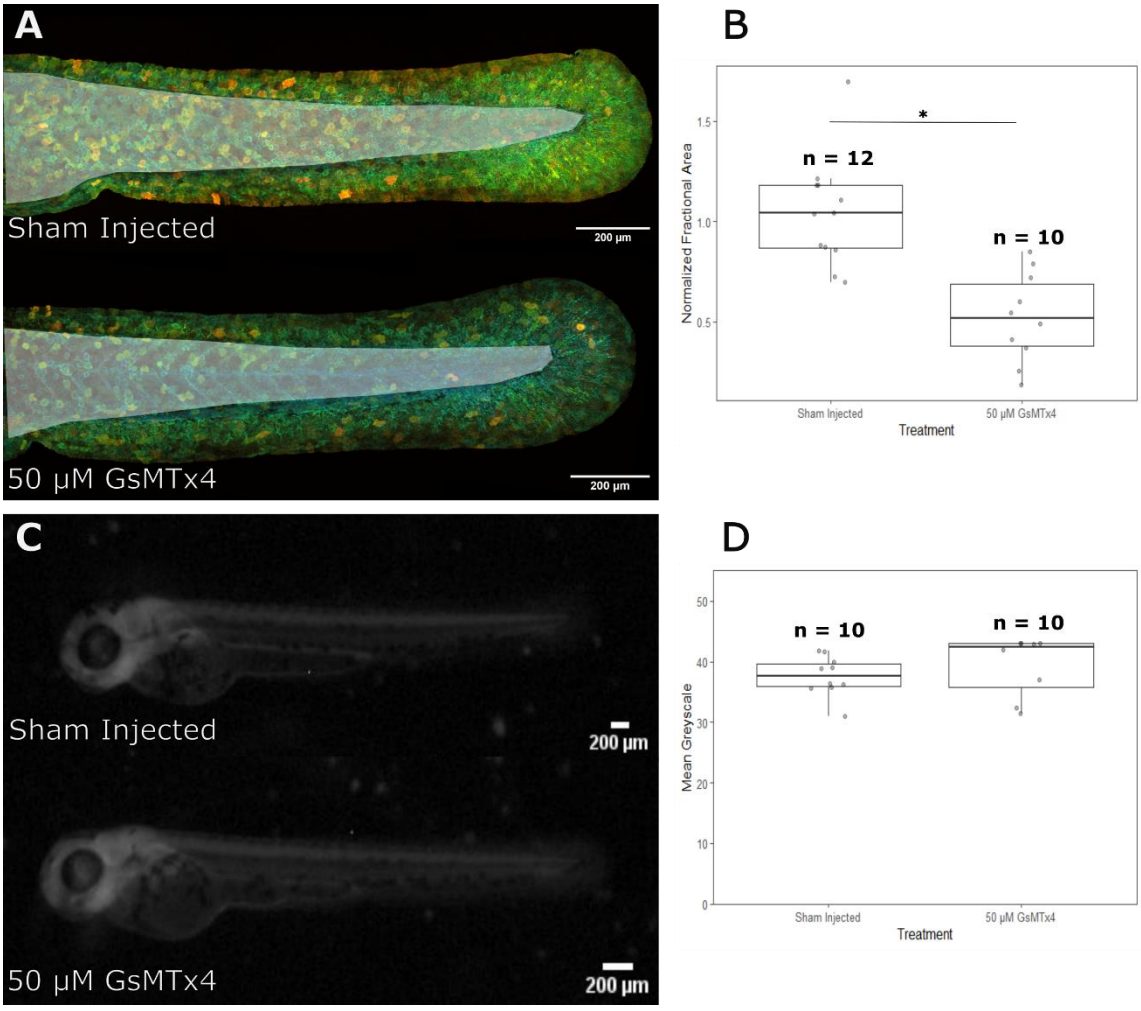

Figure 3-3: Decreasing Piezo1 activity results in reduced activation of EMMA-Mmp2. A) Composite confocal projection of EMMA-processed 72 hpf embryos microinjected with danieau buffer (top) or 50 µM GsMTx4 (bottom). Shaded area indicates area excluded from quantification. **B)** Quantification of EMMA-Mmp2 activation in the epidermis using colour thresholding ($p < 0.001$, $t = 4.948$, d.f. = 19.999, mean (sham injected) = 1.041 ± 0.272, mean (50 µM GsMTx4) = 0.520 ± 0.223). **C)** Live 72 hpf embryos microinjected with danieau buffer (top) or 50 µM GsMTx4 (bottom). **D)** Quantification of GFP intensity obtained by measuring mean greyscale values ($p = 0.422$, $t = -0.832$, d.f. = 11.508, mean (sham injected) = 37.637 ± 3.251, mean (50 µM GsMTx4) = 39.341 ± 5.003).

Piezo1 is best known for being a calcium channel but it is also permeable to other ions, so I wanted to verify that activation of EMMA-Mmp2 is sensitive to calcium signalling. I treated embryos with the calcium ionophore A23187, finding that embryos

bathed in A23187 show significantly increased EMMA-Mmp2 activation in the epidermis (Figure 3-4). There was no significant difference in the expression of the EMMA-Mmp2 transgene between A23187-treated embryos and control embryos.

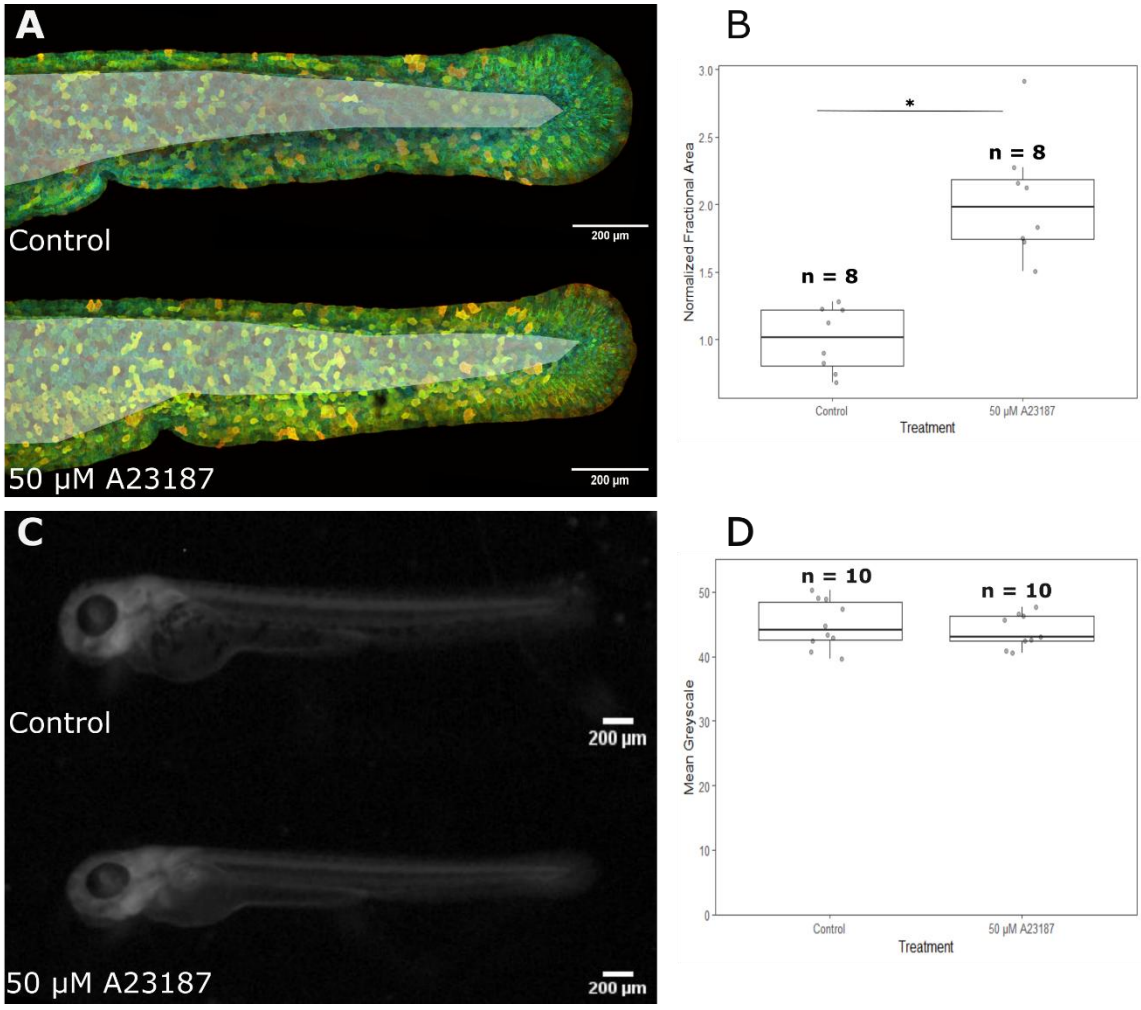

Figure 3-4: Calcium signalling increases activation of EMMA-Mmp2. A) Composite confocal projection of EMMA-processed 72 hpf embryos bathed in vehicle control (top) or 50 µM A23187 (bottom). Shaded area indicates area excluded from quantification. **B)** Quantification of EMMA-Mmp2 activation in the epidermis using colour thresholding ($p < 0.001$, $t = -5.849$, d.f. = 10.817, mean (control) = 1.000 ± 0.239, mean (50 µM A23187) = 2.036 ± 0.440). **C)** Live 72 hpf embryos bathed in vehicle control (top) or 50 µM A23187 (bottom). **D)** Quantification of GFP intensity obtained by measuring mean greyscale values ($p = 0.515$, $t = 0.666$, d.f. = 16.105, mean (control) = 44.939 ± 3.718, mean (50 µM A23187) = 43.965 ± 2.605).

3.2 *mmp14b* expression is altered by Piezo1 activity

While linking mechanical signalling to the post-translational activation of Mmp2 is exciting progress in understanding how tissue remodeling is may be regulated by morphogenetic forces, the molecular mechanisms linking Piezo1 signalling (which increases intracellular calcium) and Mmp2 activation (which occurs extracellularly) remain obscure. Mmp14 is a well-known activator of Mmp2 (Strongin, 1993; Murphy 2016), so I next wanted to determine if Piezo1 signalling has an effect on *mmp14b* expression.

I bathed wild-type embryos with Yoda1 and used HCR to determine whether increasing Peizo1 activity increases expression of *mmp14b*. I found that embryos bathed in Yoda1 have significantly increased *mmp14b* expression compared to control embryos (Figure 3-5 A&B). Conversely, embryos microinjected with GsMTx4 express *mmp14b* at lower levels compared to sham injected embryos (Figure 3-6 A&B). To verify that the chemical treatments were specifically altering *mmp14b* expression, I bathed wild-type embryos with Yoda1, microinjected embryos with GsMTx4, and used HCR to determine whether altering Piezo1 activity changes the expression of other genes expressed in the fin-fold epidermis. For these experiments I chose *keratin 4 (krt4)*, a gene encoding an intermediate filament protein that is expressed in epidermal cells. For both Yoda1-bathed embryos and GsMTx4-microinjected embryos there was no significant difference in *krt4* expression between treatment and control embryos (Figure 3-5 C&D; Figure 3-6 C&D).

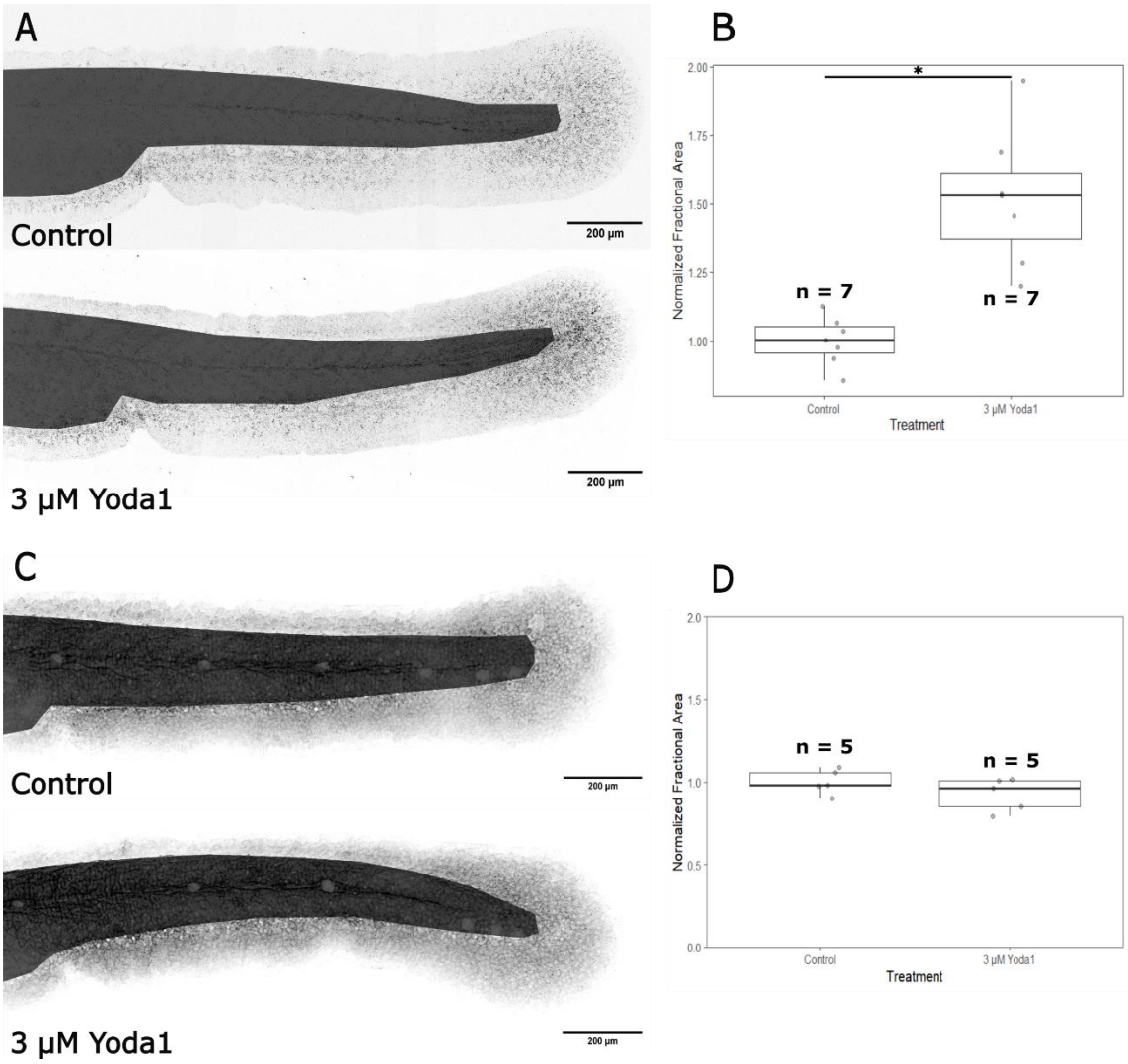

Figure 3-5: Increasing Piezo1 activity increases *mmp14b* expression. A) Composite confocal projection of HCR-RNA-FISH 72 hpf embryos bathed in vehicle control (top) or 3 µM Yoda1 (bottom). Shaded area indicates area excluded from quantification. **B)** Quantification of *mmp14b* expression in the epidermis using thresholding (p = 0.001, t = -5.192, d.f. = 7.482, mean (control) = 1.000 ± 0.089, mean (3 µM Yoda1) = 1.521 ± 0.250). **C)** Composite confocal projection of HCR-RNA-FISH 72 hpf embryos bathed in vehicle control (top) or 3 µM Yoda1 (bottom). Shaded area indicates area excluded from quantification. **D)** Quantification of *krt4* expression in the epidermis using thresholding (p = 0.223, t = 1.332, d.f. = 7.317, mean (control) = 1.000 ± 0.074, mean (3 µM Yoda1) = 0.926 ± 0.101).

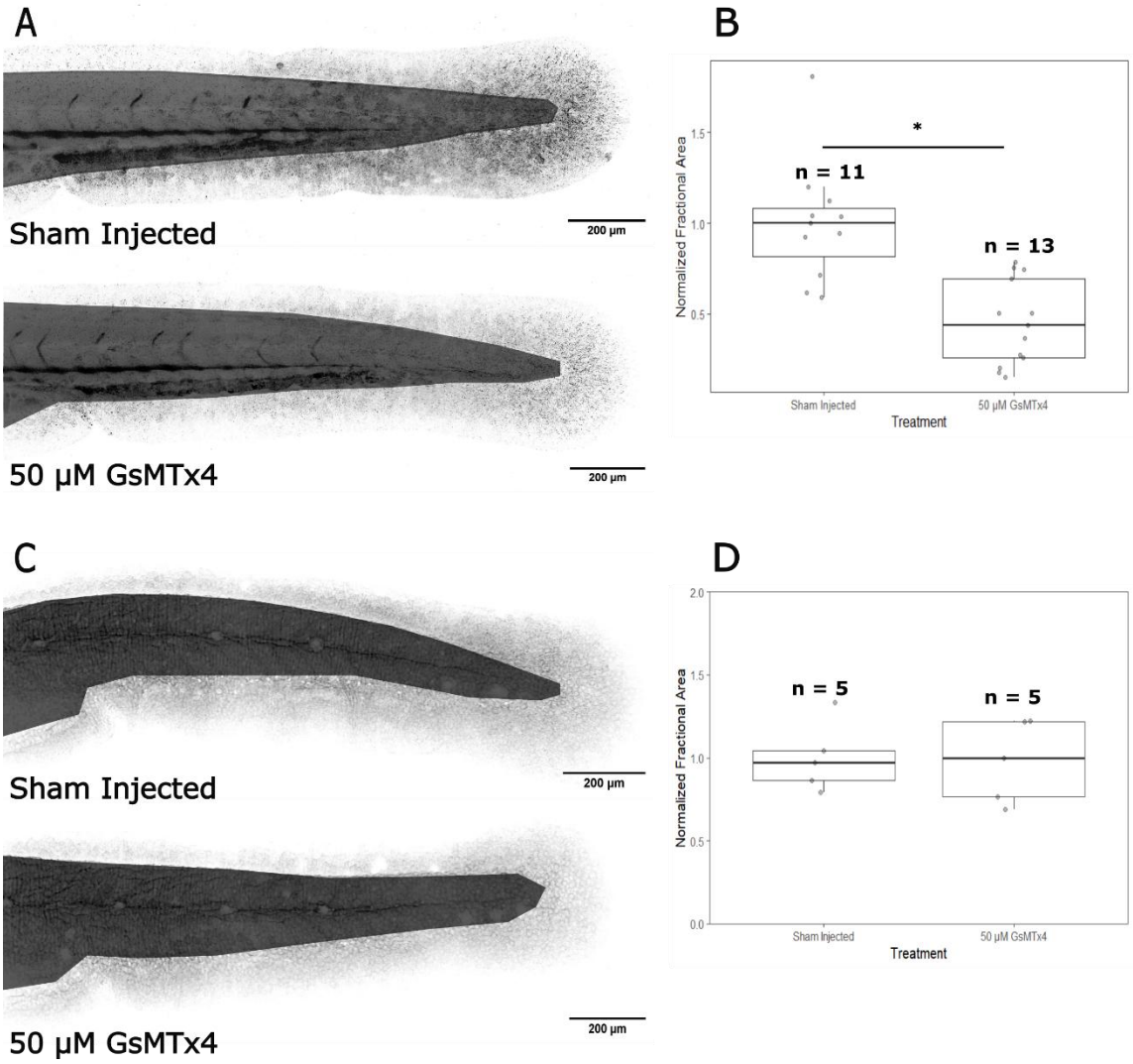

Figure 3-6: Decreasing Piezo1 activity reduces *mmp14b* expression. A) Composite confocal projection of HCR-RNA-FISH 72 hpf embryos microinjected with danieau buffer (top) or 50 µM GsMTx4 (bottom). Shaded area indicates area excluded from quantification. **B)** Quantification of *mmp14b* expression in the epidermis using thresholding ($p < 0.001$, $t = 4.580$, d.f. = 17.476, mean (control) = 1.000 ± 0.335, mean (50 µM GsMTx4) = 0.451 ± 0.234). **C)** Composite confocal projection of HCR-RNA-FISH 72 hpf embryos microinjected with danieau buffer (top) or 50 µM GsMTx4 (bottom). Shaded area indicates area excluded from quantification. **D)** Quantification of *krt4* expression in the epidermis using thresholding ($p = 0.879$, $t = 0.158$, d.f. = 7.802, mean (control) = 1.000 ± 0.211, mean (50 µM GsMTx4) = 0.977 ± 0.247).

3.3 Erk inhibition reduces EMMA-Mmp2 activation and *mmp14b* expression

Because ERK activity increases expression of MT1-MMP (Takino *et al*., 2004), I suspected the MAP kinase cascade might be playing a role in Piezo1-dependent activation of Mmp2 via Mmp14. To test this, I used the MEK/ERK pathway inhibitor PD0325901, which inhibits the activation and downstream signalling of MEK thereby supressing the phosphorylation (activation) of MEK's only known target: ERK (Ciuffreda *et al*., 2009; Anastasaki *et al*., 2012). I used both the EMMA assay and HCR to characterize the effects of Erk inhibition on Mmp2 activation and *mmp14b* expression. Consistent with mechanical signalling through Piezo1 activating Erk, I observed decreased activation of EMMA-Mmp2 in embryos treated with PD0325901 (Figure 3-7), as well as reduced expression of *mmp14b* (Figure 3-8). There was no significant difference in GFP intensity or *krt4* expression between embryos treated with PD0325901 and control embryos.

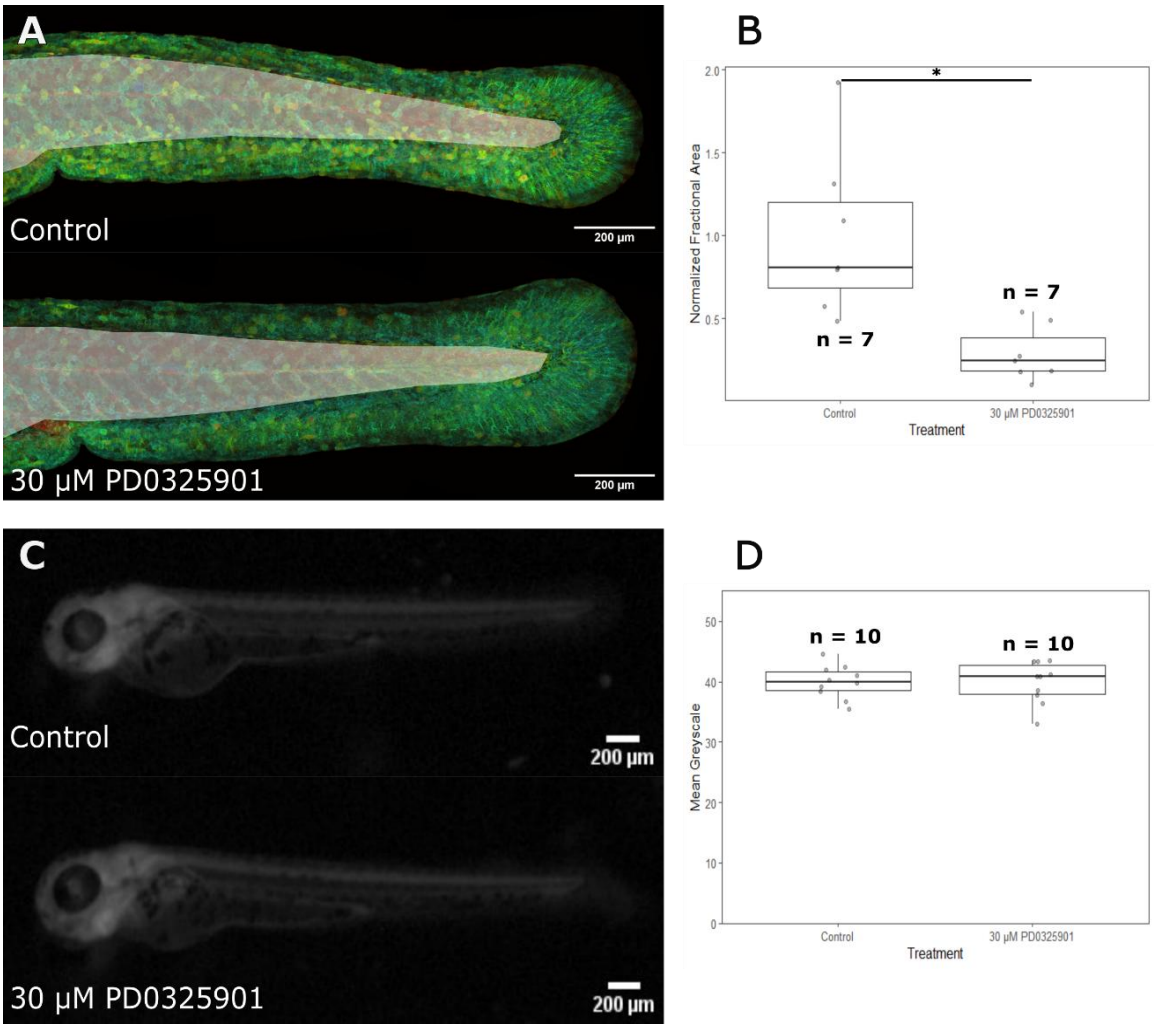

Figure 3-7: Inhibiting Mek/Erk signalling reduces EMMA-Mmp2 activation. A) Composite confocal projection of EMMA-processed 72 hpf embryos bathed in vehicle control (top) or 30 µM PD0325901 (bottom). Shaded area indicates area excluded from quantification. **B)** Quantification of EMMA-Mmp2 activation in the epidermis using colour thresholding ($p = 0.008$, $t = 3.587$, d.f. = 7.319, mean (control) = 1.000 ± 0.497, mean (30 µM PD0325901) = 0.290 ± 0.166). **C)** Live 72 hpf embryos bathed in vehicle control (top) or 30 µM PD0325901 (bottom). **D)** Quantification of GFP intensity obtained by measuring mean greyscale values ($p = 0.966$, $t = 0.043$, d.f. = 17.005, mean (control) = 39.954 ± 2.711, mean (30 µM PD0325901) = 39.894 ± 3.469).

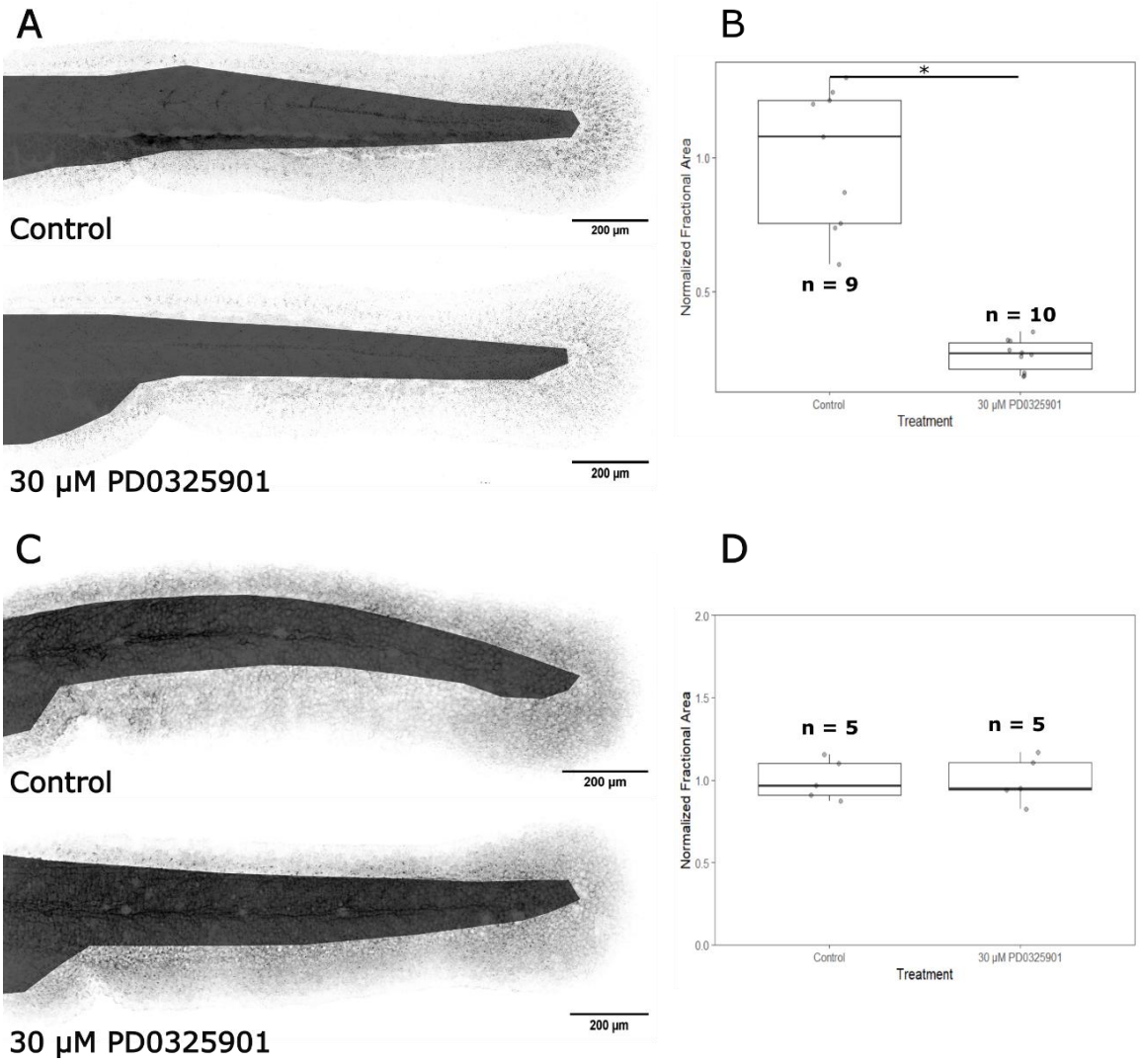

Figure 3-8: Inhibiting Mek/Erk signalling reduces *mmp14b* expression. A) Composite confocal projection of HCR-RNA-FISH 72 hpf embryos bathed in vehicle control (top) or 30 µM PD0325901 (bottom). Shaded area indicates area excluded from quantification. **B)** Quantification of *mmp14b* expression in the epidermis using thresholding ($p < 0.001$, $t = 8.264$, d.f. = 8.722, mean (control) = 1.000 ± 0.262, mean (30 µM PD0325901) = 0.262 ± 0.059). **C)** Composite confocal projection of HCR-RNA-FISH 72 hpf embryos bathed in vehicle control (top) or 30 µM PD0325901 (bottom). Shaded area indicates area excluded from quantification. **D)** Quantification of *krt4* expression in the epidermis using thresholding ($p = 0.968$, $t = 0.042$, d.f. = 7.881, mean (control) = 1.000 ± 0.122, mean (30 µM PD0325901) = 0.997 ± 0.139).

3.4 Trapping embryos in their chorion biases stretching of the epidermis

To demonstrate that the activation of EMMA-Mmp2 is the result of mechanical signalling, I trapped embryos in their chorion by bleaching at 24 hpf, causing increased crosslinking of the ZP proteins, thereby reducing hatching efficiency (Hall *et* al., 2023). Embryos trapped within their chorion were still able to move; however, they tend to be dorsally extended and ventrally compressed. I predicted that this would cause increased mechanical stretching of the epidermis in the tail dorsally and that these embryos would therefore have higher EMMA-Mmp2 activation in the dorsal epidermis compared to the ventral epidermis. I found that 30% of embryos trapped in their chorions exhibited increased EMMA-Mmp2 activation dorsally, with a dorsal/ventral ratio of EMMA-Mmp2 activation of 144.9, 21.7, and 6.6. All other trapped embryos had a dorsal/ventral ratio less than 1.3. No control embryos had a dorsal/ventral ratio greater than 1.3 (Figure 3-9). In embryos that were trapped in their chorion, all embryos showed decreased expression of EMMA-Mmp2 overall (i.e., lower brightness) compared to dechorionated control embryos. Considering this possible confounding factor and the small sample size, I did not perform any statistical tests.

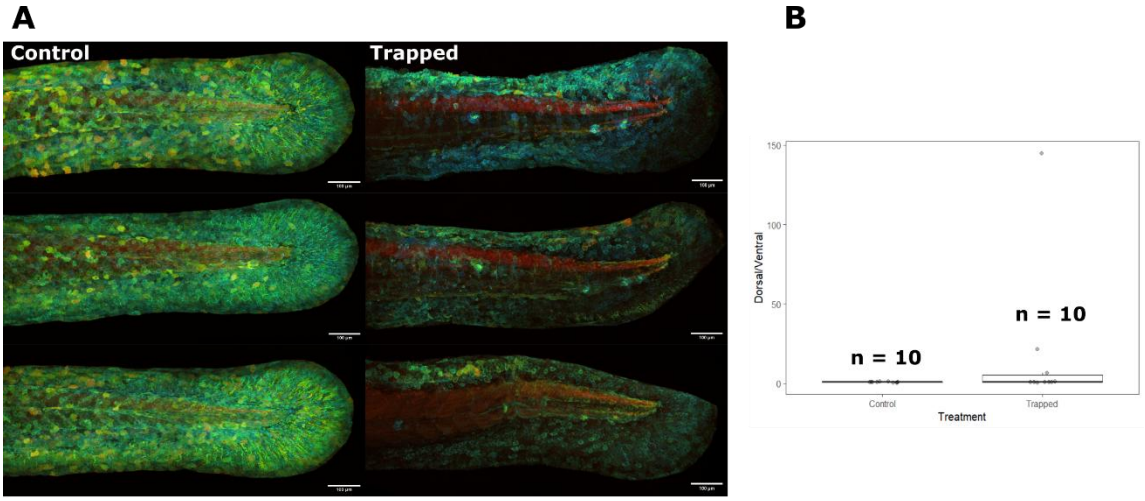

Figure 3-9: EMMA-Mmp2 activation is increased by stretch in the epidermis. A) Composite confocal projections of the tails of EMMA-processed 72 hpf embryos that had undergone normal hatching (left) or had been trapped in their chorions until processing (right). Scale bars = 100 µM. **B)** Ratios of relative activation in dorsal vs. ventral epidermis in ten replicates from each group (higher = more activation dorsally).

3.5 RT gelatin zymography

To verify that the observed changes in the proteolytic processing of the EMMA-Mmp2 reporter in the context of altered Piezo1 signalling are consistent with changes in the activation of the endogenous Mmp2 protein, I made homogenates of wildtype embryos treated with 3 µM Yoda1 and 30 µM PD0325901 and quantified the amount of endogenous active Mmp2 versus inactive Mmp2 using RT gelatin zymography (Figure 3-10). In embryos treated with 3 µM Yoda1, I see a slight increase in the proportion of active Mmp2 compared to control embryos; however, due to the low sample size I did not perform any statistical tests. In embryos treated with 30 µM PD0325901, there was no observed qualitative change in the proportion of active Mmp2 compared to control embryos. In both the PD0325901 control and 30 µM PD0325901 lanes, the signal-to-noise ratio was very high making it difficult to distinguish the inactive from the active bands. I also see significant breakdown of Mmp2 in the PD0325901 control and 30 µM

PD0325901 lanes, as well as protein contamination in lane 7 (Figure 3-10).

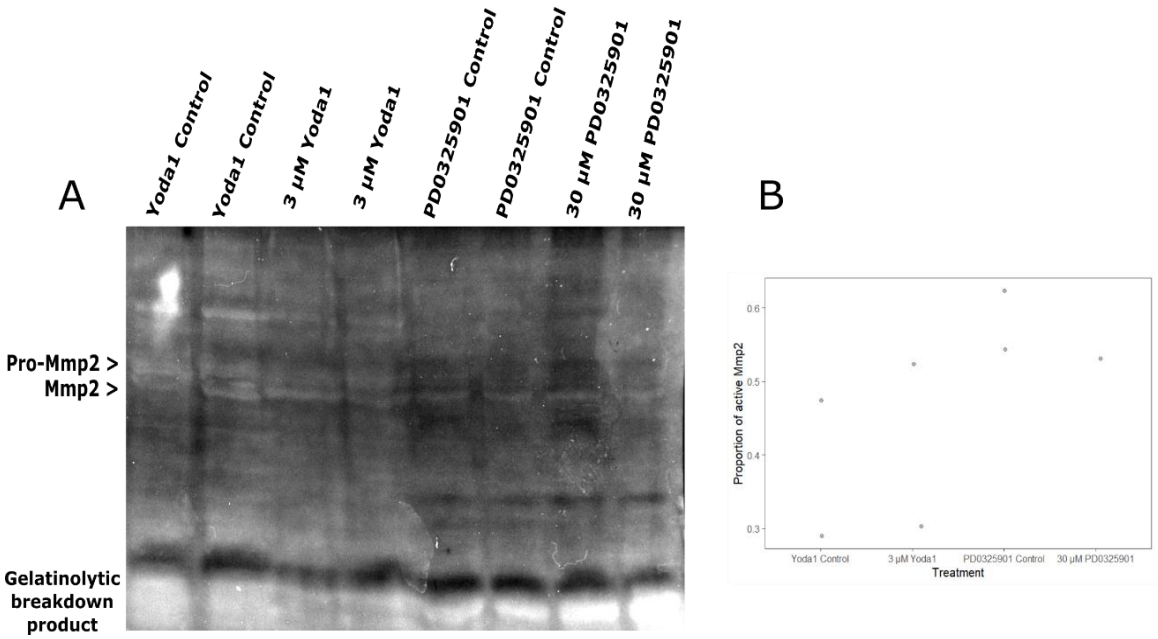

Figure 3-10: Endogenous Mmp2 activation is increased slightly in embryos treated with Yoda1. A) Real time gelatin zymography of 72 hpf embryo homogenates bathed in Yoda1 vehicle control (lanes 1 & 2), 3 µM Yoda1 (lanes 3 & 4), PD0325901 vehicle control (lanes 5 & 6), or 30 µM PD0325901 (lanes 7 & 8). **B)** Quantification of the proportion of active Mmp2 using densitometry. Lane 7 was excluded due to protein contamination.

4. Discussion

The gelatinases are the best studied of the MMPs, but there is relatively little known about their post-translational regulation *in vivo*. The epitope-mediated MMP activation (EMMA) assay is a tool to study and better understand the post-translational activation of Mmp2 and other MMPs in intact living tissues.

In the epidermis of growing embryos Mmp2 activation is patchy, with individual or small groups of neighbouring cells activating Mmp2 while other cells nearby show little to no activation (Wyatt & Crawford, 2021). Other experiments using fluorogenic MMP substrates *in vivo* and embryos injected with molecular beacons bearing hydroxamic acid groups designed to bind the exposed sites of active MMPs also reveal a patchy pattern of MMP activity/exposed active sites (Keow *et al*., 2011; Keow *et al*., 2012). Here, I show that this patchy pattern of EMMA-Mmp2 activation occurs in response to signalling through the stretch-activated Piezo1 mechanoreceptor, resulting in Erk-mediated expression of *mmp14b*. This novel mechanism links the biomechanical forces experienced by tissues in developing embryos with the biochemical mechanisms controlling that morphogenetic ECM remodeling (Figure 4-1).

It has long been known that calcium signalling activates the ERK pathway (Chunderland & Seger, 2008), and ERK activation through Piezo1 has recently been demonstrated *in vitro* (Sugimoto *et al*., 2023). In tissue culture models, Piezo1 signalling is implicated in sensing matrix stiffness and the activation of epithelial-to-mesenchymal transition (He *et al*., 2022; Lopez-Cavestany *et al*., 2023), and in the activation of MMP14 expression during angiogenesis (Kang *et al*., 2019). *In vitro* studies also suggest that MMP-14 activates ERK through an unknown mechanism, which in turn increases

mmp14 expression and MMP-14 presentation on the plasma membrane, with a corresponding increase in MMP-2 activation (Takino *et al*., 2004). Very recently Ramkumar *et al.* demonstrated that stretch in the epidermis of zebrafish embryos activates Erk, activating cellular proliferation *in vivo* (2025). These results are consistent with my findings that mechanical signalling via Piezo1 and calcium activate Erk, resulting in activation of matrix metalloproteinases, facilitating matrix remodelling.

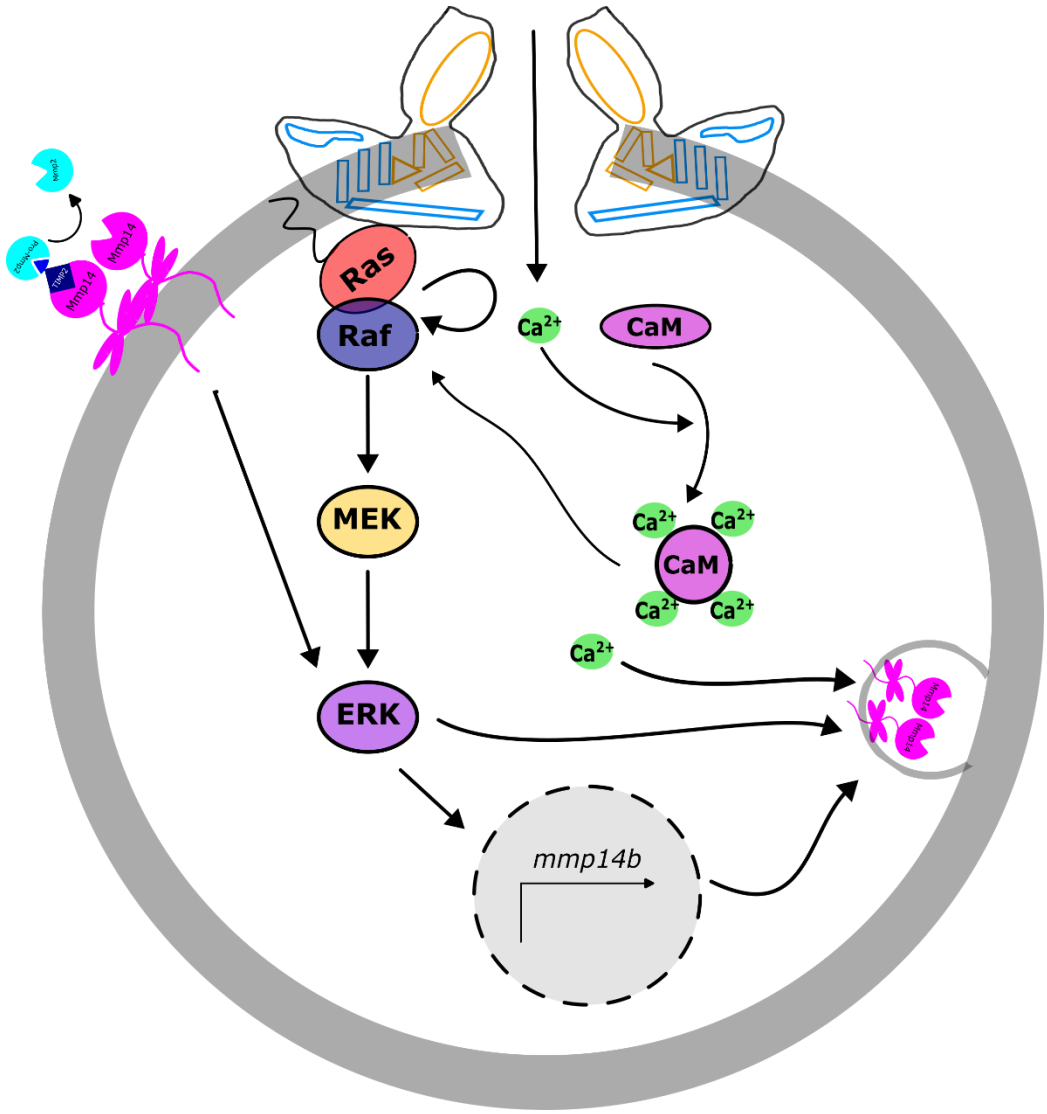

Figure 4-1: Proposed pathway of Piezo1-dependent activation of Mmp2 via Mmp14 and Erk signalling. Piezo1 calcium signalling activates the Erk cascade. Mmp14 activates Erk which in turn upregulates *mmp14* expression and Mmp14 presentation on the cell surface, resulting in increased processing of Mmp2.

In addition to the changes in EMMA-Mmp2 activation and *mmp14b* expression I see using chemical modifiers of Piezo1 activity, I also observe increased EMMA-Mmp2 activation in the dorsal epidermis of embryos trapped in their chorion compared to the ventral epidermis. While this is something never observed in embryos that have hatched from their chorion, I am cautious to draw conclusions from this experiment. In all trapped

embryos the overall expression of the EMMA-Mmp2 construct is decreased. This is likely because trapped embryos were experiencing oxidative stress from reduced oxygen availability through the hardened chorion. I also only saw increased EMMA-Mmp2 activation dorsally in 30% of trapped embryos. This is likely due to embryos still being able to move and flip within their chorions, even while trapped. Additional mechanical manipulations are needed to verify these results.

I also show using real-time gelatin zymography that activation of Piezo1 using Yoda1 appears to increase endogenous active Mmp2. More replicates are needed to assess the significance of this observed increase; however, because I conducted these assays on homogenates of whole embryos, and given that Yoda1 treatment is applied via bathing, it is likely that limited drug penetration is limiting the exposure of the drug to the epidermis. It is also possible that significant stretch is only being experienced in the epidermis at this stage of development. Given that the proportion of Mmp2 sourced from the epidermis is likely small and I would not expect bathing in Yoda1 to affect Mmp2 activation throughout the embryo, it is likely the increased activation of Mmp2 in the epidermis is being diluted by the rest of the Mmp2 present in these samples. Using the EMMA assay, I can restrict my quantification of Mmp2 activation to the epidermis, eliminating the issues of drug penetration and Mmp2 elsewhere in the embryo being subject to other regulatory regimes, providing me with greater confidence in these results.

Despite the potential for Piezo1 signalling to be a general mechanism for MMP activation and matrix remodelling, it cannot be the only pathway regulating this ubiquitous ECM remodeling effector. This is evident in the normal development of Piezo mutant zebrafish (Ramli *et al*., 2024). This is also consistent with my results: embryos

treated with the Piezo1 antagonist GsMTx4 show reduced but not abolished activation of EMMA-Mmp2, and treatment with Yoda1 increases EMMA-Mmp2 activation, but does not result in ubiquitous activation. There must be other mechanism(s) for Mmp2 activation.

Integrins, TRP channels, nuclear deformation and the hippo signalling pathway are all involved in mechanotransduction and almost certainly contribute to MMP regulation. Integrins are heterodimeric transmembrane receptors that connect the ECM to the intracellular actin cytoskeleton (Sun *et al*., 2016). Integrins convey forces from the cytoplasm across the plasma membrane to the ECM and vice versa. Although lacking enzymatic activity themselves, integrins interact with a variety of signalling molecules through their cytoplasmic tails, including several non-receptor tyrosine kinases (e.g. focal adhesion kinase, Src, and integrin-linked kinase), allowing integrins to regulate signalling pathways in response to the mechanical cues perceived through the ECM (Katsumi *et al*., 2004). Intriguingly, integrins have recently been shown to interact with Piezo1 (Kechagia *et al*. 2019; Emig *et al*. 2021; Cheng *et al*., 2023), suggesting a possible collaborative role in the mechanical signalling system.

TRPs are a large family of ion channels that are widely distributed throughout the body. TRPs are involved in many mechanotransduction processes; however, it is still uncertain whether they sense mechanical cues directly or act downstream of primary mechanotransducers, potentially including Piezo (Yin & Kuebler, 2009; Cox *et al*., 2024). Finally, YAP (yes-associated protein) and TAZ (transcriptional coactivator with PDZ-binding motif) are transcriptional coactivators that operate as part of the mechanosensitive Hippo signalling pathway (Ortega *et al*., 2021). In environments with

stiff matrices, YAP/TAZ localize to the nucleus, indicating they are active, whereas in environments with soft matrices, YAP/TAZ localize to the cytoplasm, indicating they are inactive (Dupont *et al*., 2011). Interestingly, Erk activation is regulated by integrins, TRPs, and YAP/TAZ, as well as Piezo1, suggesting that Erk could be a central integrator of mechanical signalling (Aplin *et al*., 2001; White *et al*., 2020; Zhong *et al*., 2021), driving ECM remodeling by increasing MMP activation.

It is possible that in addition to the increased expression of *mmp14b* I see, Piezo1 calcium signalling may also increase MT1-MMP presentation on the cell surface. Calcium has long been known to trigger the fusion of vesicles with the plasma membrane (Burgoyne & Morgan, 1998). For MT1-MMP to end up on the cell surface, MT1-MMP bearing vesicles must fuse with the plasma membrane so one mechanism by which Piezo1 could be increasing Mmp2 activation is by increasing membrane presentation of MT1-MMP that was sequestered intracellularly in vesicles.

In 2004, Takino *et al*. found that increased ERK signalling increases MT1-MMP levels on the cell surface. They suggest that ERK signalling recruits TIMP-2 to form the trimolecular complex with MT1-MMP and MMP-2, which prevents the endocytosis and lysosomal degradation of MT1-MMP, thereby resulting in increased MT1-MMP protein on the cell surface (Takino *et al*., 2004). However, ERK signalling is also able to regulate exocytosis and vesicle fusion (Ren & Guo, 2012), suggesting ERK signalling may increase MT1-MMP presentation on the cell surface by increasing fusion of MT1-MMP bearing vesicles with the plasma membrane. ERK signalling regulates exocytosis and vesicle fusion by phosphorylating Exo70, a component of the exocyst complex which regulates vesicle tethering at the plasma membrane (Ren & Guo, 2012). In cells in which

ERK signalling is blocked, vesicle fusion was reduced and interestingly there was also a reduction in MMP-2 and MMP-9 secretion (Ren & Guo, 2012). This data suggests that ERK signalling may result in increased Mmp2 activation by increasing transcriptional expression of *mmp14*, increasing MT1-MMP presentation on the cell surface, decreasing removal of MT1-MMP from the cell surface, and by increasing secretion of Mmp2.

4.1 Future work & conclusions

Firstly, to verify that the changes I see in Mmp2 activation and *mmp14b* expression are due to mechanical cues, zebrafish embryos could be imbedded in agarose to prevent expansion of the mesoderm, or subjected to controlled mechanical forces by deforming the agarose in which they are embedded. This would confirm that mechanical stretch results in increased Mmp2 activation and increased *mmp14b* expression, rather than relying on chemical modulators of Piezo1 activity.

Given that integrins, TRPs, and Hippo all function as mechanotransducers, it would be interesting to examine their role in Mmp2 activation. Specific agonists and antagonists of integrins and TRPs could be used to investigate their role in the Mmp2 activation pathway as I have done here with respect to Piezo and Erk signalling modulators. While GsMTx4 is an inhibitor of both Piezo and TRP channels, there are no specific Piezo inhibitors, so it cannot be used to evaluate TRP inhibition alone. Fortunately, there are broad-spectrum but TRP-specific inhibitors that can be used, such as 2-aminoethoxydiphenyl borate (2-APB), flufenamic acid (FFA), and SKF-96365 (Bencze *et al*., 2015). Efforts to identify drugs that modulate YAP/TAZ activity have been less successful. However, a transgenic zebrafish line that reports on hippo signalling exists (Miesdelf & Link, 2014); it could be used—perhaps in conjunction with CRISPR,

morpholinos or other knockdown approaches—to investigate the effects of YAP/TAZ on Mmp2 activation. Injecting EMMA-Mmp2 embryos with a Yap morpholino (Hu *et al*., 2013) would reveal if Yap knockdown changes EMMA-Mmp2 activation. The same experiment could be done in wildtype embryos with HCR to determine if Yap knockdown also influences *mmp14b* expression.

Finally, a transgenic line of zebrafish that reports on Erk activity exists (Ramkumar *et al*., 2025). Using this reporter, along with both Yoda1 or GsMTx4, would confirm that Piezo1 activity alters Erk activity. This transgenic line could also be used with chemical modifiers of integrin and TRP activity to investigate their role in Erk activation as well.

In this thesis, I show that calcium signalling through Piezo1 increases EMMA-Mmp2 activation via increased expression of *mmp14b*. Further, this activation is dependent on Erk signalling. Increasing Piezo1 activity with the small molecule agonist Yoda1 results in increased EMMA-Mmp2 activation and increased *mmp14b* expression, whereas inhibiting Piezo1 activity decreases EMMA-Mmp2 activation and *mmp14b* expression. Inhibiting Erk activity also decreases both EMMA-Mmp2 activation and *mmp14b* expression. This provides a novel link between mechanical forces and the biochemical mechanisms controlling matrix remodelling *in vivo*. Exploring other potential mechanotransduction pathways will help further uncover the complex pathways at work during morphogenesis and in the maintenance of normal tissue architecture.

Bibliography

Alcorta-Sevillano, N., Macías, I., Infante, A., & Rodríguez, C. I. (2020). Deciphering the relevance of bone ECM signalling. *Cells*, *9*(12). doi: 10.3390/cells9122630

Ali, M. A. M., García-Vilas, J. A., Cromwell, C. R., Hubbard, B. P., Hendzel, M. J., & Schulz, R. (2021). Matrix metalloproteinase-2 mediates ribosomal RNA transcription by cleaving nucleolar histones. *FEBS Journal*, *288*(23), 6736–6751. doi: 10.1111/febs.16061

Alpin, A. E., Stewart, S. A., Assoian, R. K., & Juliano, R. L. (2001). Integrin-mediated adhesion regulates ERK nuclear translocation and phosphorylation of Elk-1. *Journal of Cell Biology*, *153*(2), 273–282. doi: 10.1083/jcb.153.2.273

Anaastasaki, C., Rauen, K. A., & Patton, E. E. (2012). Continual low-level MEK inhibition ameliorates cardio-facio-cutaneous phenotypes in zebrafish. *Disease Models & Mechanisms*, *5*(4), 546–552. doi: 10.1242/dmm.008672

Arnold, J. (2021). ggthemes: Extra Themes, Scales and Geoms for 'ggplot2'. *R package version 4.2.4*, https://CRAN.R-project.org/package=ggthemes.

Bae, C., Sachs, F., & Gottlieb. P. A. (2011). The mechanosensitive ion channel Piezo1 is inhibited by the peptide GsMTx4. *Biochemistry*, *50*(29), 6295–6300. doi: 10.1021/bi200770q

Bassiouni, W., Ali, M. A. M., & Schulz, R. (2021). Multifunctional intracellular matrix metalloproteinases: implications in disease. *The FEBS Journal*, *48*(3), 1014–1021. doi: 10.1111/febs.15701

Bassiouni, W., Valencia, R., Mahmud, Z., Seubert, J. M., & Schulz, R. (2023). Matrix metalloproteinase-2 proteolyzes mitofusin-2 and impairs mitochondrial function during myocardial ischemia-reperfusion injury. *Basic Research in Cardiology*, *118*(1), 29–20. doi: 10.1007/s00395-023-00999-y

Bencze, M., Behuliak, M., Vavřínová, A., & Zicha, J. (2015). Broad-range TRP channel inhibitors (2-APB, flufenamic acid, SKF-96365) affect differently contraction of resistance and conduit femoral arteries of rat. *European Journal of Pharmacology*, *765*, 533–540. doi: 10.1016/j.ejphar.2015.09.014

Berchtold, M. W. & Villalobo, A. (2013). The many faces of calmodulin in cell proliferation, programmed cell death, autophagy, and cancer. *Biochimica et Biophysica Acta*, *1843*, 398–435. doi: 10.1016/j.bbamcr.2013.10.021

Blascke de Mello, M. M., de Oliveira Neves, V. G., Parente, J. M., Pernomian, L., de Oliveira, I. S., Pedersoli, C. A., *et al*. (2024). Sarcoplasmic Reticulum Calcium ATPase (SERCA) proteolysis by matrix metalloproteinase-2 contributes to vascular dysfunction in early hypertension. *European Journal of Pharmacology*, *983*. doi: 10.1016/j.ejphar.2024.176981

Botello-Smith, W.M., Jiang, W., Zhang, H. *et al.* (2019). A mechanism for the activation of the mechanosensitive Piezo1 channel by the small molecule Yoda1. *Nature communications, 10*. doi: 10.1038/s41467-019-12501-1

Bres, E. E., & Faissner, A. (2019). Low density receptor-related protein 1 interactions with the extracellular matrix: More than meets the eye. *Frontiers in Cell and Developmental Biology*, *7*(MAR), 31. doi: 10.3389/fcell.2019.00031

Burgoyne, R. D. & Morgan, A. (1998). Calcium sensors in regulated exocytosis. *Cell Calcium, 24*(5/6), 367–376. doi: 10.1016/S0143-4160(98)90060-4

Cheng, D., Wang, J., Yao, M., & Cox, D. C. (2023). Joining forces: crosstalk between mechanosensitive PIEZO1 ion channels and integrin-mediated focal adhesions. *Biochemical Society Transactions, 51*, 1897–1906. doi: 10.1042/BST20230042

Choi, H. M. T., Schwarzkopf, M., Fornace, M. E., Acharya, A., Artavanis, G., Stegmaier, J., Cunha, A., & Pierce, N. A. (2018). *HCR™ RNA-FISH protocol for whole-mount zebrafish embryos and larvae (Danio rerio)* (v3.0). Molecular Instruments.

Chouhan, G., Lewis, N. S., Ghanekar, V., Ainavarapu, S. R. K., Inamdar, M. M., & Sonawane, M. (2024). Cell-size-dependent regulation of Ezrin dictates epithelial resilience to stretch by countering myosin-II-mediated contractility. *Cell Reports*, *43*. doi: 10.1016/j.celreo.2024.114271

Chunderland, D. & Seger, R. (2008). Calcium regulates ERK signalling by modulating its protein-protein interactions. *Communicative & Integrative Biology, 1*(1), 4–5. doi: 10.4161/cib.1.1.6107

Ciuffreda, L., Del Bufalo, D., Desideri, M., Di Sanza, C., Stoppacciaro, A., Ricciardi, M. R., Chiaretti, S., Tavolaro, S., Benassi, B., Bellacosa, A., Foà, R., Tafuri, A., Cognetti, F., Anichini, A., Zupi, G., & Milella, M. (2009). Growth-inhibitory and antiangiogenic activity of the MEK inhibitor PD0325901 in malignant melanoma with or without BRAF mutations. *Neoplasia*, *11*(8), 720–731. doi: 10.1593/neo.09398

Cox, C. D., Poole, K., & Martinac, B. (2024). Re-evaluating TRP channel mechanosensitivity. *Trends in Biochemical Sciences*, *49*(8), 693–702. doi: 10.1016/j.tibs.2024.05.004

Cox, T. R. & Erler, J. T. (2011). Remodeling and homeostasis of the extracellular matrix: implications for fibrotic disease and cancer. *Disease Models & Mechanisms*, *4*(2), 165-178. doi: 10.1242/dmm.004077

Curry, T. E. & Osteen, K. G. (2003). The matrix metalloproteinase system: changes, regulation, and impact throughout the ovarian and uterine reproductive cycle. *Endocrine Reviews*, *24*(4), 428–465. doi: 10.1210/er.2002-0005

De Almeida, L. G. N., Thode, H., Eslambolchi, Y., Chopra, S., Young, D., Gill, S., Devel, L., & Dufour, A. (2022). Matrix metalloproteinases: From molecular mechanisms to physiology, pathophysiology, and pharmacology. *Pharmacological Reviews*, *74*(3), 714–770. doi: 10.1124/pharmrev.121.000349

Di Nubila, A., Dilella, G., Simone, R., & Barbieri, S. S. (2024). Vascular extracellular matrix in atherosclerosis. *International Journal of Molecular Sciences*, *25*(22). doi: 10.3390/ijms252212017

Drobnik, M., Smólski, J., Grądalski, L., Niemirka, S., Mlynasrska, E., Rysz, J., & Franczyk, B., (2024). Mechanosensitive cation channel Piezo1 is involved in renal fibrosis induction. *International Journal of Molecular Sciences*, *25*. doi: 10.3390/ijms25031718

Dufour, A., Sampson, N. S., Zucker, S., & Cao, J. (2009). Role of the hemopexin domain of matrix metalloproteinases in cell migration. *Journal of Cellular Physiology*, *217*(3), 643–651. doi: 10.1002/jcp.213535

Dupont, S., Morsut, L., Aragona, M., Enzo, E., Giulitti, S., Cordenonsi, M., Zanconato, F., Le Digabel, J., Forcato, M., Bicciato, S., Elvassore, N., & Piccolo, S. (2011). Role of YAP/TAZ in mechanotransduction. *Nature*, *474*, 179–183. doi: 10.1038/nature10137

Emig, R., Knodt, W., Krussig, M. J., Zgierski-Johnston, C. M., Gorka, O., Gross, O., et al. (2021). Piezo1 Channels Contribute to the Regulation of Human Atrial Fibroblast Mechanical Properties and Matrix Stiffness Sensing. *Cells*, *10*(3), 663. doi: 10.3390/cells10030663

Ermakov, Y. A., Kamaraju, K., Sengupta, K., & Sukharev, S. (2010). Gadolinium ions block mechanosensitive channels by altering the packing and lateral pressure of anionic lipids. *Biophysical Journal*, *98*, 1018-1027. doi: 10.1016/j.bpj.2009.11.044

Fallata, Wyatt, Levesque, Dufour, Overall, & Crawford. (2019). Intracellular Localization in Zebrafish Muscle and Conserved Sequence Features Suggest Roles for Gelatinase A Moonlighting in Sarcomere Maintenance. *Biomedicines*, *7*(4), 93–15. doi: 10.3390/biomedicines7040093

Gaide Chevronnay, H. P., Selvais, C., Emonard, H., Galant, C., Marbaix, E., & Henriet, P. (2012). Regulation of matrix metalloproteinases activity studied in human endometrium as a paradigm of cyclic tissue breakdown and regeneration. *Biochimica Et Biophysica Acta*, *1824*(1), 146–156. doi: 10.1016/j.bbapap.2011.09.003

Gioia, M., Fasciglione, G. F., Sbardella, D., Sciandra, F., Casella, M., Camerini, S., *et al*. (2018). The enzymatic processing of α-dystroglycan by MMP-2 is controlled by two anchoring sites distinct from the active site. *PloS One*, *13*(2), e0192651–19. doi: 10.1371/journal.pone.0192651

Gisabella, B., Babu, J., Valeri, J., Rexrode, L., & Pantazopoulos, H. (2021). Sleep and memory consolidation dysfunction in psychiatric disorders: Evidence for the involvement of extracellular matrix molecules. *Frontiers in Neuroscience*, *15*. doi: 10.3389/fnins.2021.646678

Giusti, I., D'Ascenzo, S., Millimaggi, D., Taraboletti, G., Carta, G., Franceschini, N., Pavan, A., & Dolo, V. (2008). Cathepsin B mediates the pH-dependent proinvasive activity of tumor-shed microvesicles. *Neoplasia*, *10*(5), 481–488. doi: 10.1593/neo.08178

Gnanasambandam, R., Ghatak, C., Yasmann, A., Nishizawa, K., Sachs, F., Ladokhin, A. S., Sukharev, S. I., & Suchyna, T. M. (2017). GsMTx4: Mechanisms of inhibiting mechanosensitive ion channels. *Biophysical Journal*, *112*, 31–24. doi: 10.1016/j.bpj.2016.11.013

Gudipaty, S. A., Lindblom, J., Loftus, P. D., Redd, M. J., Edes, K., Davey, C. F., Krishnegowda, V., & Rosenblatt, J. (2017). Mechanical stretch triggers rapid epithelial cell division through Piezo1. *Nature*, *453*, 118–121. doi: 10.1038/nature21407

Guo, Y. R. & MacKinnon, R. (2017). Structure-based membrane dome mechanism for Piezo mechanosensitivity. *eLife*, *6*. doi: 10.7554/eLife.33660

Hadler-Olsen, E., Solli, A. I., Hafstad, A., Winberg, J.-O., & Uhlin-Hansen, L. (2015). Intracellular MMP-2 activity in skeletal muscle is associated with type II fibers. *Journal of Cellular Physiology*, *230*(1), 160–169. doi: 10.1002/jcp.24694

Hadler-Olsen, E. & Winberg, J-O. (2019). Method for determining gelatinolytic activity in tissue extracts: Real-time gelatin zymography. *The Extracellular Matrix: Methods and Protocols*, *1952*, 201–209. doi: 10.1007/978-1-4939-9133-4_16

Hall, T. E., Ariotti, N., Lo, H. P., Rae, J., Ferguson, C., Martel, N., Lim, Y-W., Giacomotto, J., & Parton, R. G. (2023). Cell surface plasticity in response to shape change in the whole organism. *Current Biology*, *33*, 4276–4284. doi: 10.1016/j.cub.2023.08.068

He, J., Shan, S., Li, Q., Fang, B., & Xie, Y. (2022). Mechanical stretch triggers epithelial-mesenchymal transition in keratinocytes through Piezo1 channel. *Frontiers in Physiology*, *13*. doi: 10.3389/fphys.2022.745572

Honoré, E., Martins, J. R., Penton, D., Patel, A., & Demolombe, S. (2015). The Piezo mechanosenstive ion channels: May the force be with you!. *Reviews of Physiology, Biochemistry and Pharmacology*, *169*, 25–42. doi: 10.1007/112_2015_26

Hu, J., Sun, S., Jiang, Q., Sun, S., Wang, W., Gui, Y., & Song, H. (2013). Yes-associated protein (Yap) is required for early embryonic development in zebrafish (Danio rerio). *International Journal of Biological Sciences*, *9*(3), 267–278. doi: 10.7150/ijbs.4887

Hu, M., Ling, Z. & Ren, X. (2022). Extracellular matrix dynamics: tracking in biological systems and their implications. *J Biol Eng*, *16*, 13. doi: 10.1186/s13036-022-00292-x

Huang, J-J., Wang, C-W., Liu, Y., Zhang, Y-Y., Yang, N-B., Yu, Y-C., Jiang, Q., Song, Q-F., & Qian, G-Q. (2023) Role of the extracellular matrix in COVID-19. *World Journal of Clinical Cases*, *11*(1), 73–83. doi: 10.12998/wjcc.v11.i1.73

Jacob-Ferreira, A. L. & Schulz, R. (2013). Activation of intracellular matrix metalloproteinase-2 by reactive oxygen-nitrogen species: Consequences and therapeutic strategies in the heart. *Archives of Biochemistry and Biophysics*, *540*(1-2), 82–93. doi: 10.1016/j.abb.2013.09.019

Jefferey, E. J. & Crawford, B. D. (2018). The epitope-mediated MMP activation assay: detection and quantification of the activation of Mmp2 in vivo in the zebrafish embryo. *Histochemistry and Cell Biology*, *149*, 277–286. doi: 10.1007/s00418-018-1634-4

Jobin, P. G., Butler, G. S., & Overall, C. M. (2017). New intracellular activities of matrix metalloproteinases shine in the moonlight. *BBA - Molecular Cell Research*, *1864*(11), 2043–2055. doi: 10.1016/j.bbamcr.2017.05.013

Kang, H., Hong, Z., Zhong, M., Klomp, J., Bayless, K. J., Mehta, D., Karginov, A. V., Hu, G., & Malik, A. B. (2019). Piezo1 mediates angiogenesis through activation of MT1-MMP signalling. *American Journal of Physiology. Cell Physiology*, *316*, C92–C103. doi: 10.1152/ajpcell.00346.2018

Katsumi, A., Orr, A. W., Tzima, E., & Schwartz, M. A. (2004). Integrins in mechanotransduction. *Journal of Biological Chemistry*, *279*(13), 12001–12004. doi: 10.1074/jbc.R300038200

Kechagia, J. Z., Ivaska, J., & Roca-Cusachs, P. (2019). Integrins as biomechanical sensors of the microenvironment. *Nature Reviews Molecular Cell Biology*, *20*(8), 457–473. doi: 10.1038/s41580-019-0134-2

Keow, J. Y, Herrmann, K. M., & Crawford, B. D. (2011) Differential *in vivo* zymography: A method for observing matrix metalloproteinase activity in the zebrafish embryo. *Matrix Biology*, *30*(3), 169–177. doi: 10.1016/j.matbio.2011.01.003

Keow, J. Y, Pond, E. D., Cisar, J. S., Cravatt, B. F., & Crawford, B. D. (2012). Activity-based labeling of matrix metalloproteinases in living vertebrate embryos. *PLoS One*, *7*(8), e43434. doi: 10.1371/journal.pone.00343434

Laronha, H. & Caldeira, J. (2020). Structure and function of human matrix metalloproteinases. *Cells*, *9*(5). doi: 10.3390/cells9051076

Lee, T., Esemuede, N., Sumpio, B. E., & Gahtan, V. (2003). Thrombospondin-1 induces matrix metalloproteinase-2 activation in vascular smooth muscle cells. *Journal of Vascular Surgery*, *38*(1), 147–154. doi: 10.1016/s0741-5214(02)75468-2

Lopez-Cavestany, M., Hahn, S. B., Hope, J. M., Reckhorn, N. T., Greenlee, J. D., Schwager, S. C., VanderBurgh, J. A., Reinhart-King, C. A., & King, M. R. (2023). Matrix stiffness induces epithelial-to-mesenchymal-transition via Piezo1-regulated calcium flux in prostate cancer cells. *iScience*, *26*(4), 106275. doi: 10.1016/j.isci.2023.106275

Madzharova, E., Kastl, P., Sabino, F., & Keller, U. (2019). Post-translational modification-dependent activation of matrix metalloproteinases. *International Journal of Molecular Sciences*, *20*(3077), 11–28. doi:10.3390/ijms20123077

Mason, S. D. & Joyce, J. A. (2011). Proteolytic networks in cancer. *Trends in Cell Biology*, *21*(4), 228–237. doi: 10.1016/j.tcb.2010.12.002

Martinac, B. (2022). 2021 Nobel Prize for mechanosensory transduction. *Biophysical Reviews*, *14*(1), 15–20. Doi: 10.1007/s12551-022-00935-9

Maybee, D., Cromwell, C., Hubbard, B., & Ali, M. (2023, June 8). MMP-2 regulates Src activation via repression of the CHK/MATK tumor suppressor in Osteosarcoma. *Authorea Preprints*. Authorea. doi: 10.22541/au.168624020.08576588/v1

Meng, N., Li, Y., Zhang, H., & Sun, X.-F. (2008). RECK, a novel matrix metalloproteinase regulator. *Histology and Histopathology*, *23*(8), 1003–1010. doi: 10.14670/HH-23.1003

Miyagawa, T., Hasegawa, K., Aoki, Y., Watanabe, T., Otagiri, Y., Arasaki, K., Wakana, Y., Asano, K., Tanaka, M., Yamaguchi, H., Tagaya, M., & Inoue, H. (2019). MT1-MMP recruits the ER-Golgi SNARE Bet1 for efficient MT1-MMP transport to the plasma membrane. *Journal of Cell Biology*, *218*(10), 3355–3371. doi: 10.1083/jcb.201808149

Monea, S., Lehti, K., Keski-Oja, J., & Mignatti, P. (2002). Plasmin activates pro-matrix metalloproteinase-2 with a membrane-type 1 matrix metalloproteinase-dependent mechanism. *Journal of Cellular Physiology*, *192*(2) 160–170. doi: 10.1002/jcp.10126

Mukhopadhyay, S., Munshi, H. G., Kambhampati, S., Sassano, A., Platanias, L. C., & Stack, M. S. (2004). Calcium-induced matrix metalloproteinase 9 gene expression is differentially regulated by ERK1/2 and p38 MAPK in oral keratinocytes and oral squamous cell carcinoma. *Journal of Biological Chemistry*, *279*(32), 33139–33146. doi: 10.1074/jbc.M405194200

Munshi, H. G., Wu, Y. I., Ariztia, E. V., & Stack, M. S. (2002). Calcium regulation of matrix-metalloproteinase-mediated migration in oral squamous cell carcinoma cells. *Journal of Biological chemistry*, *277*(44), 41480–41488. doi: 10.1074/jbc.M207695200

Murphy, G. (2016). Matrix Metalloproteinases. *Encyclopedia of Cell Biology* (621-629). doi: 10.1016/B978-0-12-394447-4.10073-2

Musale, V., Wasserman, D. H., & Kang, L. (2023). Extracellular matrix remodelling in obesity and metabolic disorders. *Life Metabolism*, *2*(4). doi: 10.1093/lifemeta/load021

Nagase, H., Ogata, Y., Suzuki, K., Enghild, J. J., & Salvesen, G. (1991). Substrate specificities and activation mechanisms of matrix metalloproteinases. *Biochem Soc Trans*, *19*(3), 715–718. doi: 10.1042/bst0190715.

Nishida, Y., Miyamori, H., Thompson, E. W., Takino, T., Endo, Y., & Sato, H. (2008). Activation of matrix metalloproteinase-2 (MMP-2) by membrane type 1 matrix metalloproteinase through an artificial receptor for proMMP-2 generates active MMP-2. *Cancer Research*, *68*(21), 9096–9104. doi: 10.1158/0008-5472.CAN-08-2522

Ortega, A., Vera, I., Diaz, M. P., Navarro, C., Rojas, M., Torres, W., Parra, H., Salazar, J., De Sanctis, J. B., & Bermúdez, V. (2021). The YAP/TAZ signalling pathway in the tumor microenvironment and carcinogenesis: Current knowledge and therapeutic promises. *International Journal of Molecular Sciences*, *23*(1). doi: 10.3390/ijms23010430

Pickup, M. W., Mouw, J. K., & Weaver, V. M. (2014). The extracellular matrix modulates the hallmarks of cancer. *EMBO Reports*, *15*(12), 1243–1253. doi: 10.15252/embr.201439246

Prakriya, M. (2021). Calcium and cell function. *Journal of Physiology*, *589*(9), 1647-1648. doi: 10.1113/JP279541

Preibisch, S., Saalfeld, S., & Tomancak, P. (2009). Globally optimal stitching of tiled 3D microscopic image acquisitions. *Bioinformatics*, *25*(11), 1463–1465. doi: 10.1093/bioinformatics/btp184

Qin, L., He, T., Chen, S., Yang, D., Yi, W., Cao, H., & Xioa, G. (2021). Roles of mechanosensitive channel Piezo1/2 proteins in skeleton and other tissues. *Bone Research*, *9*(44). doi: 10.1038/s41413-021-00168-8

Ra, H. J. & Parks, W. C. (2007). Control of matrix metalloproteinase catalytic activity. *Matrix biology: journal of the International Society for Matrix Biology*, *26*(8), 587–596. doi: 10.1016/j.matbio.2007.07.001

Ramkumar, N., Richardson, C., O'Brien, M., Butt, F. A., Park, J., Chao, A. T., Bagnat, M., Poss, K. D., & Di Talia, S. (2025). Phased ERK responsiveness and developmental robustness regulate teleost skin morphogenesis. *PNAS*, *122*(10), e24110430122

Ramli, Aramaki, T., Watanade, M., & Kondo, S. (2024). Piezo1 mutant zebrafish as a model of idiopathic scoliosis. *Frontiers in Genetics*, *8*(4): 1321379. doi: 10.3389/fgene.20231321379

R Core Team (2023). R: A Language and Environment for Statistical Computing. *R Foundation for Statistical Computing*, Vienna, Austria. https://www.R-project.org/

Ren, J. & Guo, W. (2012). ERK1/2 regulate exocytosis through direct phosphorylation of the exocyst component Exo70. *Developmental Cell*, *22*(5), 967–978. doi: 10.1016/j.devcel.2012.03.005

Resnikoff, H. A., Miller, C. G., & Schwarzbauer, J. E. (2022) Implications of fibrotic extracellular matrix in diabetic retinopathy. *Experimental Biological Medicine*, *247*(13), 1093–1102. doi: 10.1177/15353702221087175

Salzano, M., Rusclano, M. R., Bifulco, M., Postiglione, L., & Vitale, M. (2012). Calcium/calmodulin-dependent protein kinase II (CaMKII) phosphorylates Raf-1 at serine 338 and mediates Ras-stimulated Raf-1 activation. *Cell Cycle*, *11*(11), 2100–2106. doi: 10.4161/cc.20543

Schindelin, J., Arganda-Carreras, I., Frise, E., Kaynig, V., Longair, M., Pietzsch, T., … Cardona, A. (2012). Fiji: an open-source platform for biological-image analysis. *Nature Methods*, *9*(7), 676–682. doi:10.1038/nmeth.2019

Sekiguchi, R. & Yamada, K. M. (2018). Basement membranes in development and disease. *Current Topics in Developmental Biology*, *130*, 144–191. doi: 10.1016/bs.ctdb.2018.02.005

Silver, F. H., Siperko, L. M., & Seehra, G. P. (2003). Mechanobiology of force transduction in dermal tissue. *Skin Research and Technology*, *9*(1), 3–23. doi: 10.1034/j.1600-0846.2003.00358.x

Sounni, N. E., Rozanov, D. V., Remacle, A. G., Golubkov, V. S., Noel, A., Strongin, A. Y. (2011). Timp-2 binding with cellular MT1-MMP stimulates invasion-promoting MEK-ERK signalling in cancer cells. *International Journal of Cancer*, *126*(5), 1067–1078. doi: 10.1002/ijc.24690

Strongin, A. Y., Marmer, B. L., Grant, G. A., & Goldberg, G. I. (1993). Plasma membrane-dependent activation of the 72-kDa type IV collagenase is prevented by complex formation with TIMP-2. *Journal of Biological Chemistry, 268*(19), 14033–14039.

Sugimoto, A., Iwata, K., Kurogoushi, R., Tanaka, M., Nakashima, Y., Yamakawa, Y., Oishi, A., Yoshizaki, K., Fukumoto, S., Yamamoto, A., Ishimaru, N., & Iwamoto, T. (2023). C-terminus of Piezo1 governs Ca^{2+} influx and intracellular ERK1/2 signalling pathway in mechanotransduction. *Ciochemical and biophysical research communications, 682*, 39–45. doi: 10.1016/j.bbrc.2023.09.080

Sun, Y., Xu, S., Jiang, M., Liu, X., Yang, L., Bai, Z., & Yang, Q. (2021). Role of the extracellular matrix in Alzheimer's disease. *Frontiers in Aging Neuroscience, 13*. doi: 10.3389/fnagi.2021.707466

Sun, Z., Guo, S. S., & Fässler, R. (2016) Integrin-mediated mechanotransduction. *Journal of Cell Biology, 215*(4), 445–456. doi: 10.1083/jcb.201609037

Swulius, M. T. & Waxham, M. N. (2008). Ca^{2+}/Calmodulin-dependent protein kinases. *Cellular and Molecular Life Sciences, 65*, 2637-2657. doi: 10.1007/s00018-008-8086-2

Syeda, R., Xu, J., Dubin, A. E., Coste, B., Mathur, J., Huynh, T., Matzen, J., Lao, J., Tully, D. C., Engels, I. H., Petrassi, H. M., Schumacher, A. M., Montal, M., Bandell, M., & Patapoutian, A. (2015). Chemical activation of the mechantranduction channel Piezo1. *eLife, 4e07369*. doi: 10.7554/eLife.07369

Takino, T., Miyamori, H., Watanabe, Y., Yoshioka, K., Seiki, M., & Sato, H. (2004). Membrane type 1 matric metalloproteinase regulates collagen-dependent mitogen-activated protein/extracellular signal-related kinase activation and cell migration. *Cancer Research, 64*(3), 1044–1049. doi: 10.1158/0008-5472.CAN-03-1843

Taminura, S., Asato, K., Fujishiro, S., & Kohno, M. (2003). Specific blockade of the ERK pathway inhibits the invasiveness of tumour cells: down-regulation of matrix metalloproteinase-3/-9/-14 and CD44. *Biochemical and Biophysical Research Communications, 304*(4), 801–806. doi: 10.1016/S0006-291X(03)00670-3

Tochowicz, A., Goettig, P., Evans, R., Visse, R., Shitomi, Y., Palmisano, R., *et al*. (2011). The dimer interface of the membrane type I matrix metalloproteinase hemopexin domain. *Journal of Biological Chemistry, 286*(9), 7587–7600. doi: 10.1074/jbc.M110.178434

Wagner, M. F. M. G., Theodoro, T. R., Filho, C. D. A. S. M., Oyafuso, L. K. M., & Pinhal, M. A. S. (2021). Extracellular matrix alterations in the skin of patients affected by psoriasis. *BMC Molecular and Cell Biology*, *22*(55). doi: 10.1186/s12860-021-00395-1

Wei, Q., Zhu, X., Wang, L., Zhang, W., Yang, X., & Wei, W. (2023). Extracellular matrix in synovium development, homeostasis and arthritis disease. *International Immunopharmacology*, *121*. doi: 10.1016/j.intimp.2023.110453

White, S. M., Avantaggiati, M. L., Nemazanyy, I., Di Poto, C., Yang, Y., Pende, M., Gibney, G. T., Ressom, H. W., Field, J., Atkins, M. B., & Yi, C. (2019). YAP/TAZ inhibition induces metabolic and signalling rewiring resulting in targetable vulnerabilities in *NF2*-deficient tumor cells. *Developmental Cell*, *49*(3), 425–443. doi: 10.1016/j.devcel.2019.04.014

Wickham, H. (2016). ggplot2: Elegant Graphics for Data Analysis. *Springer-Verlag*, New York, https://ggplot2.tidyverse.org

Wortzel, I. & Seger, R. (2011). The ERK cascade. *Genes & Cancer*, *2*(3), 195–209. doi: 10.1177/1947601911407328

Wyatt, R. A. (2020). *Patterns and mechanisms of post-translational regulation of Mmp2 in vivo during zebrafish development* [Doctoral dissertation, University of New Brunswick].

Wyatt, R. A. & Crawford, B. D. (2021). Post-translational activation of Mmp2 correlates with patterns of active collagen degradation during the development of the zebrafish tail. *Developmental Biology*, *477*, 155–163. doi: 10.1016/j.ydbio.2021.05.016

Xie, Y., Yerlan, P., Orakov, A. N., & Miao, L. (2017). Nuclear matrix metalloproteinases: Functions resemble the evolution from the intracellular to the extracellular compartment. *Cell Death Discovery*, *3*(1), 1–8. doi: 10.1038/cddiscovery.2017.36

Yin, K. & Kuebler, W. M. (2009). Mechanotranduction by TRP channels: General concepts and specific role in the vasculature. *Cell Biochemistry and Biophysics*, *56*, 1–18. doi: 10.1007/s12013-009-9067-2

Zhang, H. J., Zhao, W., Venkataraman, S., Robbins, M. E. C., Buettner, G. R., Kregel, K. C., & Oberley, L. W. (2002). Activation of matrix metalloproteinase-2 by overexpression of manganese superoxide dismutase in human breast cancer MCF-7 cells involves reactive oxygen species. *The Journal of Biological Chemistry*, *277*(23), 20919–20926. doi: 10.1074/jbc.M109801200

Zhang, X., Zhao, Y., LI, M., Wang, M., Qian, J., Wang, Z., Wang, Y., Wang, F., Guo, K., Gao, D., Xhao, Y., Chen, R., Ren, Z., Song, H., & Cui, J. (2023). A synergistic regulation works in matrix stiffness-driven invadopodia formation in HCC. *Cancer Letters*, *582*. doi: 10.1016/j.canlet.2023.216597

Zhong, T., Zhang, W., Guo, H., Pan, X., Chen, X., He, Q., Yang, B., & Ding, L. (2021). The regulatory and modulatory roles of TRP family channels in malignant tumors and relevant therapeutic strategies. *Acta Pharmaceutica Sinica B*, *12*(4), 1761–1780. doi: 10.1016/j.apsb.2021.11.001

Curriculum Vitae

Candidate's Full Name: Jillian E. Hickey

Universities Attended:

2025, University of New Brunswick, MSc Biology

2022, University of New Brunswick, BSc (Hons) Biology-Chemistry

Conference Presentations:

(2025). Post-translational activation of Mmp2 by Mmp14 is triggered by mechanical signalling through Piezo1 and Erk during embryonic growth in zebrafish. Conference of the Biological Sciences, Fredericton, Canada

(2024). Piezo1-mediated detection of mechanical force regulates post-translational activation of matrix metalloproteinase-2 (Mmp2) through Mmp14 in growing zebrafish embryos. Developmental Biology Symposium, Halifax, Canada

(2024). Piezo1-mediated detection of mechanical force regulates post-translational activation of matrix metalloproteinase-2 (Mmp2) in growing zebrafish embryos. Conference of the Biological Sciences, Fredericton, Canada.

(2024). Piezo1-mediated detection of mechanical force regulates post-translational activation of matrix metalloproteinase-2 (Mmp2) in growing zebrafish embryos. Canadian Society of Zoologists 63rd Annual Meeting, Moncton, Canada.

(2023). Piezo1-mediated detection of mechanical force regulates post-translational activation of matrix metalloproteinase-2 (Mmp2) in growing zebrafish embryos. Cell Bio 2023, Boston, United States of America.

(2022). Piezo1-mediated detection of mechanical force regulates post-translational activation of matrix metalloproteinase-2 (Mmp2) in growing zebrafish embryos. International Zebrafish Conference, Montreal, Canada.

(2022). Piezo1-mediated detection of mechanical force regulates post-translational activation of matrix metalloproteinase-2 (Mmp2) in zebrafish embryos. Developmental Biology Symposium, Halifax, Canada.

(2022). The Piezo1 stretch-sensitive calcium channel regulates morphogenetic post-translational activation of Mmp2 in the zebrafish embryo. Joint Pan-American Society for Evolutionary Developmental Biology and 81st Society for Developmental Biology Meeting, Vancouver, Canada.

(2022). Mechanical activation of the stretch-sensitive calcium channel Piezo1 regulates activation of matrix metalloproteinase-2 (Mmp2) in zebrafish. Science Atlantic Biology and Aquaculture Conference, Online, Canada.